

INSTITUTE FOR FUSION STUDIES

DOE/ET/53088-456

IFSR #456

A Kinetic Theory of Trapped Electron Driven Drift Wave
Turbulence in a Sheared Magnetic Field

F. Y. Gang

Institute for Fusion Studies
The University of Texas at Austin
Austin, Texas 78712

P. H. Diamond and M. N. Rosenbluth

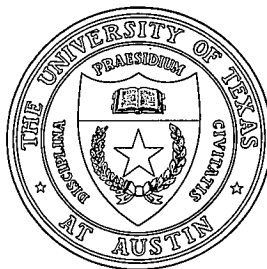
Department of Physics B-019
University of California, San Diego
La Jolla, California 92093

and

General Atomics, Inc.
San Diego, California 92138

September 1990

THE UNIVERSITY OF TEXAS



AUSTIN

A Kinetic Theory of Trapped Electron Driven Drift Wave Turbulence in a Sheared Magnetic Field

F. Y. Gang^{a)}

Institute for Fusion Studies
University of Texas at Austin
Austin, TX 78712

P. H. Diamond and M. N. Rosenbluth

Department of Physics B-019
University of California, San Diego
La Jolla, CA 92093

and

General Atomics, Inc
San Diego, CA 92138

Abstract

A kinetic theory of collisionless and dissipative trapped electron driven drift wave turbulence in a sheared magnetic field is presented. Weak turbulence theory is employed to calculate the nonlinear electron and ion responses and to derive a wave kinetic equation that determines the nonlinear evolution of trapped electron mode turbulence. Saturated fluctuation spectrum is calculated using the condition of nonlinear saturation. The turbulent transport coefficients (D , χ_i , χ_e) are in turn calculated using saturated fluctuation spectrum. Due to the disparity in the three different radial scale lengths of the slab-like eigenmode: Δ (trapped electron layer width), x_t (turning point width) and x_i (Landau damping point), $\Delta < x_t < x_i$, we find that ion Compton scattering rather than trapped electron Compton scattering is the dominant nonlinear saturation mechanism. Ion Compton scattering transfers wave energy from short to long wavelengths where the wave energy is shear damped. As a consequence, a saturated fluctuation spectrum $|\phi|^2(k_\theta) \sim k_\theta^{-\alpha}$ ($\alpha=2$ and 3 for the dissipative and collisionless regime, respectively) occurs for $k_\theta \rho_s < 1$ and is heavily damped for $k_\theta \rho_s > 1$. The predicted fluctuation level and transport coefficients are

^{a)} present address: Department of Physics B-019, University of California, San Diego, La Jolla, Ca 92093

well below the 'mixing length' estimate. This is due to the contribution of radial wavenumbers $x_i^{-1} < k_r \leq \rho_i^{-1}$ to the nonlinear couplings, the effect of radial localization of trapped electron response to a layer of width Δ , and the weak turbulence factor $\langle \frac{\gamma_e^i}{\omega_k} \rangle_{\bar{k}} < 1$, which enters the saturation level.

I Introduction

Trapped electron driven drift wave turbulence, both dissipative and collisionless, is considered to be an important agent for anomalous transport in tokamaks. While the linear theory of trapped electron instabilities has been extensively investigated,¹⁻³ the nonlinear dynamics of trapped electron drift wave turbulence remains rather poorly understood. Indeed, with relatively few exceptions,⁴⁻⁷ most previous studies of trapped electron driven drift wave turbulence have forsaken realistic geometries in favor of shearless slab models,⁸ adopted the fluid ion approximation ab initio,^{9,10} and have ignored the nonlinear dynamics of trapped electrons by a priori invocation of the “ $i\delta$ ” representation of the non-adiabatic electron response.⁸ The purpose of this investigation is to explore the theory of trapped electron drift wave turbulence, with special attention focused on the role of ion kinetic effects in the nonlinear dynamics and on the role of trapped electron nonlinearity. In order to elucidate the fundamental physics issues, we adopt the comparatively simple, albeit unrealistic, model of sheared slab geometry with magnetically trapped electrons. This model ignores the poloidal harmonic couplings induced by ion curvature drifts, and thus describes only the short wavelength, slab-like branch of trapped electron drift wave turbulence. The nonlinear theory of the long wavelength, toroidicity induced branch will be discussed in a future publication. It should be noted however, that despite the absence of shear damping of the toroidicity induced mode, it is not clear whether the slab or toroidal branch is more important agent for anomalous transport, since conventional mixing length estimates suggest that the thermal transport coefficient (in the dissipative regime, for example) for the slab branch is $\chi_{slab} \simeq \sqrt{\epsilon} \langle k_{\theta} \rho_s \rangle_{rms} \frac{\rho_s^2 c_s^2}{\nu_{eff} L_n^2} \sqrt{\frac{L_s}{L_n}}$, while for the toroidal branch is $\chi_{tor} \simeq \sqrt{\epsilon} \frac{\rho_s^2 c_s^2}{\nu_{eff} L_n^2}$.

A key feature of trapped electron driven drift wave turbulence in a sheared slab is the disparity between the three radial scales Δ , x_t , and x_i which parametrize a trapped electron eigenmode. Specifically, the three scales are: i.) the separation of adjacent mode rational surfaces for fixed toroidal mode number n , $\Delta = \frac{1}{k_{\theta} s}$. Δ is also the trapped

electron layer width, which demarks the region in which the trapped electron response is significant. Δ arises as a consequence of the fact that trapped electrons tend to bounce along magnetic field lines (i.e. $h_n^e \sim e^{-inq\theta} \tilde{h}_n^e$, where h_n^e is the nonadiabatic part of trapped electron distribution perturbation, q is the safety factor) while drift waves tend to localize at mode rational surfaces ($\phi_n \sim \sum_m e^{im\theta} \phi_m$). ii.) the turning point width $x_t = \sqrt{\frac{L_s}{L_n}} \rho_s$, where L_s , L_n , and ρ_s are the magnetic shear length, equilibrium density scale length, and ion larmor radius computed using the electron temperature. x_t demarks the extent of the region over which the Pearlstein-Berk¹¹ outgoing wave eigenmode is non-oscillatory, i.e. for $\phi_{\vec{k}} = \exp\{-i\mu \frac{x^2}{2}\}$ with $\mu = x_t^{-2}$, and is defined by the asymptotic balance of the ion polarization drift $\rho_s^2 \frac{\partial^2 \phi_{\vec{k}}}{\partial x^2}$ with the ion acoustic response $\frac{k_{\parallel}^2 c_s^2}{\omega^2} \phi_{\vec{k}}$, where k_{\parallel} is the parallel wavenumber and c_s is the ion acoustic speed. More generally, x_t is the scale at which the drift wave changes character from a quasi-two dimensional “convective cell” to a radially propagating outgoing wave. Thus, nonadiabatic electron effects contributes only for $x < x_t$, and x_t is generally assumed to be the “mixing length” for slab-like electron drift wave turbulence (i.e. the effective *mode* width). iii.) the ion Landau damping point $x_i = (\frac{L_s}{L_n}) \sqrt{\frac{T_e}{T_i}} \rho_s$, where T_e and T_i are the electron and ion temperature, respectively. x_i defines the scale at which the outgoing wave is damped by ion Landau resonance (i.e. when $\omega = k_{\parallel} v_i$). Thus, x_i characterizes the radial width of the *spectrum* $|\phi_{\vec{k}}|^2$ of drift wave turbulence, in that if $\phi_{\vec{k}} = \exp(-i\mu \frac{x^2}{2}) f(\frac{x}{x_i})$, with $x_i^2 \mu \gg 1$, the fast variation cancels upon calculating $|\phi_{\vec{k}}|^2$ (i.e. $|\phi_{\vec{k}}|^2 = f^2(\frac{x}{x_i})$). It is interesting to note that for $x_t < x < x_i$, the drift wave develops large radial wave-numbers $k_r = -\mu x = -\frac{x}{x_t^2} \leq \rho_i^{-1}$. For most $k_{\theta} \rho_s$ of interest, $\Delta < x_t \ll x_i$.

Several crucial aspects of the theory of trapped electron drift wave turbulence are revealed by consideration of the scales Δ , x_t , x_i and their disparity. First, the fact that the spectrum width is given by x_i ensures that the virtual, driven modes (i.e. those driven by the beat interaction $(\omega + \omega', \vec{k} + \vec{k}')$ of a test wave (ω, \vec{k}) and background mode (ω', \vec{k}')) are resonant, on account of the natural width of the ballistic frequency

$k'_{\parallel} v_{\parallel}$, i.e. for resonance, $\omega + \omega' \leq \Delta(k'_{\parallel} v_{\parallel})$, but $\Delta(k'_{\parallel} v_{\parallel}) \sim \omega'$, since $\Delta(k'_{\parallel}) = \frac{k'_g}{L_s} x'_i$. This observation indicates that while the fluid ion approximation may be valid for test wave dynamics, where $x < x_t$ is of greatest interest, it is a manifestly invalid description of the nonlinear interaction dynamics, since it ignores the beat-wave resonance $\omega'' \sim k''_{\parallel} v_i$ and thus fails to represent nonlinear ion Landau damping and Compton scattering. Moreover, it is interesting to note that while ion fluid mode coupling among strongly dispersive drift waves requires large amplitude dependent turbulent broadening of the three-wave frequency mismatch $\omega_{MM} \sim \omega \sim \Delta\omega$, the kinetic beat wave resonance is Doppler broadened at *infinitesimal* amplitudes by the spatial extent of the background mode spectrum x_i , i.e. $\Delta(k_{\parallel} v_i) \sim k_g/L_s x_i v_i \sim \omega$. As $\omega \geq \Delta\omega$, the Doppler broadening is the more significant one. These two observations suggest that nonlinear ion Landau damping and Compton scattering, as described by kinetic weak turbulence theory (since $\gamma < \omega_r$), are important (and likely dominant!) processes in the nonlinear dynamics of slab-like trapped electron modes. Finally, it is also worthwhile to note that since x' extends to x'_i , k'_r can approach ρ_i^{-1} . Thus, radial wavenumbers $k_r \leq \rho_i^{-1}$ contribute to the 'coupling coefficient' $\vec{k} \cdot \vec{k}' \times \vec{z}$. Since, $k'_r > x_t^{-1}$, saturation at levels $\frac{\bar{n}}{n_0}$ below the conventionally quoted 'mixing length estimated' of $\frac{\bar{n}}{n_0} \sim \frac{x_t}{L_n}$ appears likely!

A second crucial feature of trapped electron modes is the disparity between the width of the electron layer Δ on one hand and the mode width x_t and spectral width x_i (i.e. $\Delta < x_t < x_i$), on the other. This disparity underlines the dominance of ion nonlinearity over electron nonlinearity, since electron interaction is limited to $|x| < \Delta$, while the region of nonlinear ion-mediated interaction extends to x_i . Indeed, the effect of localization of trapped electron effects to a layer of width Δ has already been manifested in the linear theory² of trapped electron instabilities, where calculated linear growth rates are smaller than their local theory analogy by a factor $\frac{\Delta}{x_t} \ln \frac{x_t}{\Delta} < 1$, i.e. the ratio of the electron layer width to the mode width. Of course, in the case of toroidicity induced drift modes¹² for which the mode and the spectral widths are comparable to Δ , the nonlinear dynamics

of the collisionless trapped electrons are *not* subdominant, since the electron layer width correction factor approaches unity.

In this paper, a kinetic theory of collisionless and dissipative trapped electron drift wave turbulence is presented. A slab-like model (i.e. magnetically trapped electrons, with ion curvature effects neglected) is used throughout. Nonlinear trapped electron and ion interaction mechanisms are treated on an equal footing. A nonlinear bounce-kinetic equation is used to calculate the nonlinear (collisionless) trapped electron response perturbatively. While nonlinear trapped electron-wave interaction tends to transfer energy from long to short wavelengths, it is subdominant to the nonlinear ion-wave interaction process, since $\Delta \ll x_t, x_i$. The nonlinear ion response is also calculated perturbatively, following the standard procedures of weak turbulence theory¹³. The Doppler broadening of the beat wave resonance induced by the large ion spectral width (x_i) indicates that ion Compton scattering is a relevant and robust nonlinear interaction process. Ion Compton scattering results in spectral transfer to long wavelengths, primarily by local interaction. A power law spectrum $|\phi|^2(k_\theta) \sim k_\theta^{-\alpha}$ ($\alpha=2$ and 3 for dissipative and collisionless regimes, respectively) results, with a low- k_θ cutoff determined by the balance of linear growth with shear damping. Fluctuation levels are lower than naive mixing length prediction $\frac{\tilde{n}}{n_0} \sim \frac{x_t}{L_n}$. The calculated fluctuation spectrum is used to calculate the electron and ion thermal diffusivities, and the particle flux.

At this point it is appropriate to comment on the relation of this investigation to previous works of similar bent. Refs.(4) and (5) treat only nonlinear ion dynamics for slab-like and toroidal drift modes, respectively, and neglect electron nonlinearity, ab initio. Ref.(6) discusses nonlinear trapped electron dynamics in the context of a purely local model, which therefore ignores the disparity between Δ , x_t and x_i . Thus, the conclusions reached in that work are not universal. With regards to ion dynamics, some of the conclusions reached here concerning the relative importance of local and nonlocal transfer processes and the structure of the predicted fluctuation spectrum differ with those presented in Ref.(4). This

is, in part, due to exceedingly large value of T_e/T_i tacitly assumed in that investigation. Finally, Ref.(7) is exclusively focused on the effect of mode coupling mediated by resonant trapped electrons (i.e. trapped electron clumps) and on the resultant broadening of the frequency linewidth.

The remainder of this paper is organized as follows. In Sec.II, we discuss the model equations. In Sec.III, the linear theory of the trapped electron mode is reviewed. In Sec.IV, weak turbulence theory is employed to calculate the nonlinear ion response and the nonlinear trapped electron response. In Sec.V, we derive a wave kinetic equation which describes the nonlinear evolution of trapped electron mode turbulence. In Sec.VI, we discuss the various nonlinear wave-particle interaction mechanisms and calculate the associated nonlinear transfer rate. The complications of slab-like eigenmode structure for the nonlinear wave particle interaction are emphasized. In Sec.VII, the saturated fluctuation spectrum and fluctuation level are calculated. In Sec.VIII, the saturated fluctuation spectrum obtained in the previous section is used to calculate the ion and electron thermal transport coefficients, and the particle transport coefficient. The implications of these results to the tokamak transport are then discussed. In Sec.IX, the summary and conclusion are presented.

II: Basic Model

In this section, the basic model of trapped electron driven drift wave turbulence is discussed. We consider toroidal geometry with circular concentric magnetic surfaces, parametrized by the usual coordinates (r, θ, ξ) corresponding to the minor radius, the poloidal angle and the toroidal angle, respectively. In this coordinate system, the equilibrium magnetic field can be written as $\vec{B} = B(\vec{e}_\xi + \frac{\epsilon}{q}\vec{e}_\theta)$, where $\epsilon = \frac{r}{R_0}$ is the inverse aspect ratio, R_0 is the major radius from the magnetic axis, $B = B_0(1 - \epsilon \cos \theta)$ is the magnitude of the magnetic field, q is the safety factor, and $\vec{e}_\theta, \vec{e}_\xi, \vec{e}_r$ are the unit vectors in the poloidal, toroidal and radial directions, respectively. The equilibrium distribution

functions are assumed to be local Maxwellians, with density N and temperature T_j , i.e.

$$F_j = N \left(\frac{M_j}{2\pi T_j} \right)^{\frac{3}{2}} \exp \left\{ -\frac{M_j v^2}{2T_j} \right\}, j = i, e \quad (1)$$

where M_j is the mass, v is the velocity, and j denotes the species.

For the sake of simplicity, we neglect both ion and electron temperature gradient in this analysis. We also assume that the electron temperature T_e is higher than the ion temperature T_i .

For the perturbed ion distribution function f^i and electrostatic potential perturbation ϕ , we can Fourier analyze in θ and ξ and time t ,

$$[f^i, \phi] = \sum_l [f_l^i, \phi_l] \exp \{ i(m\theta - n\xi - \omega t) \} \quad (2)$$

where $l \equiv (m, n)$, and m, n are the poloidal and toroidal mode numbers, respectively. The ion's dynamics is described by the nonlinear gyrokinetic equation,¹⁴

$$-i(\omega - k_{\parallel} v_{\parallel}) h_{\omega}^i + i \frac{e}{T_i} F_i (\omega - \omega_i^*) J_0 \left(\frac{k_{\perp} v_{\perp}}{\Omega_i} \right) \phi_{\omega} = N_{\omega} \quad (3)$$

with the nonlinear mode coupling term N_{ω} given by

$$N_{\omega} = -i \frac{c}{B} \sum_{\omega'} \left\{ k_{\theta} \frac{\partial}{\partial r} \left[J_0 \left(\frac{k'_{\perp} v_{\perp}}{\Omega_i} \right) \phi_{-\omega'} \right] h_{\omega''}^i + k'_{\theta} \frac{\partial}{\partial r} \left[J_0 \left(\frac{k'_{\perp} v_{\perp}}{\Omega_i} \right) \phi_{-\omega'} h_{\omega''}^i \right] \right\}$$

where $l'' = l + l'$, $\omega'' = \omega + \omega'$. In the above equations, h_{ω}^i is the nonadiabatic part of ion distribution perturbation in the guiding center system, and is related to f_{ω}^i through $f_{\omega}^i = -\frac{e}{T_i} F_i \phi_{\omega} + h_{\omega}^i e^{i\vec{e}_{\parallel} \cdot \frac{\vec{k}_{\perp} \times v_{\perp}}{\Omega_i}}$, \vec{e}_{\parallel} is the unit vector in the direction of the local magnetic field, Ω_i is the ion gyrofrequency, J_0 is the zeroth order Bessel function, $k_{\parallel} = \frac{1}{qR}(m - nq)$ is the parallel wavenumber, $\omega_i^* = -\frac{cT_i}{eB} \frac{k_{\theta}}{L_n}$ is the ion diamagnetic drift frequency, $k_{\theta} = \frac{m}{r}$ is the poloidal wavenumber, k_{\perp} is the perpendicular wavenumber, $\vec{k}_{\perp} = k_{\theta} \vec{e}_{\theta} + k_r \vec{e}_r$, and $k_r = -i \frac{\partial}{\partial r}$. The ion density perturbation is given by

$$\delta n_{\omega}^i = -\frac{e}{T_i} N \phi_{\omega} + \int d^3 v J_0 \left(\frac{k_{\perp} v_{\perp}}{\Omega_i} \right) h_{\omega}^i \quad (4)$$

For trapped electrons, we assume $\nu_{eff}, \omega_{De}, \omega < \omega_{be}$, where $\nu_{eff} = \frac{\nu_{ei}}{e}$ is the effective collision frequency, and ω_{De}, ω_{be} are the electron magnetic precession and bounce frequencies, respectively. In the collisionless regime, we have $\omega > \omega_{De} > \nu_{eff}$, so that the mode is destabilized by the magnetic precession resonance of high energy trapped electrons. In the dissipative regime (strong collisional regime), we have $\nu_{eff} > \omega > \omega_{De}$, so that the mode is destabilized by the collisional detrapping effect. In the intermediate collisional regime ($\omega > \nu_{eff} > \omega_{De}$), the growth rate of the mode has such a favorable temperature dependence ($\gamma_e^l \propto T_e^{-2}$) that it seems quite likely that the turbulence will eventually evolve into the collisionless regime. Therefore, in this discussion, we focus primarily on the collisionless and dissipative regime.

Since trapped electrons can induce poloidal couplings, the electron perturbed distribution function f^e and the electrostatic potential perturbation ϕ are Fourier analyzed only in ξ and t ,

$$[f^e, \phi] = \sum_{\omega} [f_{\omega}^e, \phi_{\omega}] \exp\{i(-n\xi - \omega t)\}, \quad (5)$$

The trapped electron dynamics is described by a nonlinear bounce-kinetic equation,¹⁵

$$-i(\omega - \omega_{de} + i\tilde{\nu}_{eff})\hat{h}_{\omega}^e - i\frac{e}{T_e}F_e(\omega - \omega_e^*)\langle e^{-inq\theta} \phi_{\omega} \rangle_b = N_{\omega}^e \quad (6)$$

where the nonlinear mode coupling term is

$$N_{\omega}^e = -i\frac{c}{B} \sum_{\omega'} \left\{ \frac{nq}{r} \left(\frac{\partial}{\partial r} \langle e^{in'q\theta} \phi_{-\omega'} \rangle_b \right) \hat{h}_{\omega''}^e + \frac{n'q}{r} \frac{\partial}{\partial r} \left(\langle e^{in'q\theta} \phi_{-\omega'} \rangle_b \hat{h}_{\omega''}^e \right) \right\}$$

In the above equations, \hat{h}_{ω}^e is the nonadiabatic part of the trapped electron distribution perturbation, and is related to f_{ω}^e through $f_{\omega}^e = \frac{e}{T_e}F_e\phi_{\omega} + \hat{h}_{\omega}^e e^{inq\theta}$, $\omega_{de} = \omega_{De} \frac{v^2}{v^2}$, $\omega_{De} = \frac{L_n}{R}\omega_e^*$, $\omega_e^* = \frac{cT_e}{eB} \frac{k_{\parallel}}{L_n}$, $\tilde{\nu}_{eff} = \nu_{eff}(\frac{v_{\parallel}}{v})^3$, and $\langle \dots \rangle_b \equiv [\int \frac{d\theta}{v_{\parallel}} \dots] / [\int \frac{d\theta}{v_{\parallel}}]$ denotes a bounce average. The untrapped electron is treated as adiabatic. The electron density perturbation is then given by

$$\delta n_{\omega}^e = \frac{e}{T_e}N\phi_{\omega} + \int_t d^3\tilde{\nu} \hat{h}_{\omega}^e e^{inq\theta} \quad (7)$$

where the velocity integration is over the trapped electron population only. The velocity space variables in Eqs.(4) and (7) are the velocity v , the magnetic moment $\mu = \frac{v_{\perp}^2}{2B}$ and the gyrophase angle φ . Finally, by imposing the quasineutrality condition $\delta n_m^i = \delta n_n^e$, Eqs. (3)-(4) and (6)-(7) are closed.

III. Review of linear theory

In this section, the linear theory of trapped electron mode is reviewed with attention focused on those properties that are important for an understanding of the nonlinear evolution of the mode. Included are the mode frequency, the growth rate, and the mode structure. For a detailed discussion, the reader is referred to Ref.(2). Linearizing Eq.(3) and Eq.(6), we obtain the linear responses for both ions and trapped electrons,

$$h_i^i = \frac{e}{T_i} F_i \frac{\omega - \omega_i^*}{\omega - k_{\parallel} v_{\parallel}} J_0\left(\frac{k_{\perp} v_{\perp}}{\Omega_i}\right) \phi_{\omega}^i \quad (8a)$$

$$\hat{h}_n^e = -\frac{e}{T_e} F_e \frac{\omega - \omega_e^*}{\omega - \omega_{de} + i\tilde{\nu}_{eff}} \langle e^{-inq\theta} \phi_n \rangle_b \quad (8b)$$

It is important to note that trapped electrons respond to $\langle e^{-inq\theta} \phi_n \rangle_b$, the bounce average of the projection of the potential fluctuation along the magnetic field line, rather than the potential fluctuation ϕ_n itself. In the presence of magnetic shear, the pitch of the magnetic field line is different from that of the mode, i.e., $nq(r) \neq m$, except at the mode rational surface. Away from the mode rational surface, due to its fast oscillation, the bounce average of $e^{-inq\theta} \phi_n$ tends to vanish. Therefore the trapped electron's response is radially localized with a spatial scale length much smaller than the mode width. Physically, this is equivalent to saying that the trapped electrons can only feel the potential fluctuation near mode rational surfaces, where the difference between the pitch of the magnetic field line and that of the mode is negligible. As a consequence of this radial localization effect, the growth rate of the mode is considerably reduced. The fact that trapped electrons respond to the magnetic field line rather than the mode rational surface also introduces poloidal couplings among modes which center at different mode rational surfaces. However, as pointed out by Catto and Tsang in Ref.(2), this poloidal coupling effect is rather weak.

Now, we can use Eq.(4) and Eq.(7) to calculate the ion and the electron density response. For ions the calculation is straight forward. To perform the velocity integration over the trapped electron population, we note that $d^3\vec{v} \simeq 4\pi(\frac{\epsilon}{2})^{\frac{1}{2}}v^2dv d\kappa^2(\kappa^2 - \sin^2\frac{\theta}{2})^{-\frac{1}{2}}$, where instead of using variables v and μ , we use v and κ , κ is the pitch angle variable, and is defined by $\kappa^2 = [\frac{1}{2}v^2 - \mu B_0(1 - \epsilon)]/2\epsilon\mu B_0$. We then Fourier transform δn_n^e in θ , i.e., $\delta n_n^e = \frac{1}{2\pi} \int_{-\infty}^{\infty} d\theta e^{-im\theta} \delta n_n^e$, and invert the order of the θ and κ^2 integrations by noting that $\int_{-\pi}^{\pi} d\theta \int_{\kappa_0}^1 d\kappa^2 = \int_0^1 d\kappa^2 \int_{-\theta_0}^{\theta_0} d\theta$, where $\kappa_0 = \sin\frac{\theta_0}{2}$. The final results of the calculation are,

$$\delta n_n^i = -\frac{e}{T_i} N [1 + (1 - \frac{\omega_i^*}{\omega}) \frac{\omega}{|k_{\parallel} v_i|} Z(\frac{\omega}{|k_{\parallel} v_i|}) \Gamma_0(b_i)] \phi_n^m \quad (9)$$

and

$$\delta n_n^e = \frac{e}{T_e} N (\phi_n^m + \hat{\Upsilon}_e^l \langle e^{-inq\theta} \phi_n \rangle_b) \quad (10a)$$

$$\hat{\Upsilon}_e^l \langle e^{-inq\theta} \phi_n \rangle_b = (\frac{\epsilon}{2})^{\frac{1}{2}} (1 - \frac{\omega_e^*}{\omega}) g_n \int_0^1 d\kappa^2 \overline{e^{i(nq-m)\theta}} \langle e^{-inq\theta} \phi_n \rangle_b \quad (10b)$$

In the above equations, Z is the plasma dispersion function, Γ_0 is the zeroth order modified Bessel function, $b_i = \frac{1}{2} k_{\perp}^2 \rho_i^2$, $\overline{e^{i(nq-m)\theta}}$, and g_n are defined as

$$\begin{aligned} \overline{e^{i(nq-m)\theta}} &= \int_{-\theta_0}^{\theta_0} \frac{d\theta}{2\pi} \frac{e^{i(nq-m)\theta}}{\sqrt{\kappa^2 - \sin^2\frac{\theta}{2}}} \\ g_n &= -\frac{2}{\sqrt{\pi}} \int_{t_0}^{\infty} \sqrt{t} dt \frac{e^{-t}}{1 - \frac{\omega_{Re} t}{\omega} + i \frac{\nu_e t}{\omega} t^{-\frac{1}{2}}} \end{aligned} \quad (11)$$

where $t_0 = (\frac{qR\nu_e}{\epsilon^{\frac{1}{2}} v_e})^{\frac{1}{2}} \ll 1$

Let's consider a reference mode rational surface located at r_m determined by $m = nq(r_m)$, then $k_{\parallel} = \frac{k_e}{L_s} x$, where $x = r - r_m$ is the distance from mode rational surface, $L_s = \hat{s}^{-1} qR$ is the shear length, and $\hat{s} = -\frac{d \ln q}{d \ln r}$ is the shear parameter. We define the Landau resonance point $x_i \equiv \frac{\omega}{k_{\parallel} v_i}$ where $k_{\parallel}' = \frac{k_e}{L_s}$. Then, in the spatial region $x > x_i$, the mode is heavily Landau damped. Hence, the mode exists only in the region $x < x_i$. By making the fluid ion approximation $\omega \gg k_{\parallel} v_{\parallel}$, and noting that $b_i < 1$ for $\frac{T_i}{T_e} < 1$, Eq.(9)

can be simplified to be,

$$\delta n_n^i = \frac{e}{T_e} N [\rho_s^2 \frac{\partial^2}{\partial x^2} + \frac{\omega_e^*}{\omega} - k_\theta^2 \rho_s^2 + \rho_s^2 \mu^2 x^2] \phi_n^m \quad (12)$$

where ρ_s is the ion larmor radius computed using electron temperature, and $\rho_s^2 \mu^2 = (\frac{k_\parallel c_s}{\omega})^2$.

By imposing the quasineutrality condition, we obtain the linear eigenmode equation,

$$[\rho_s^2 \frac{\partial^2}{\partial x^2} + \frac{\omega_e^*}{\omega} - k_\theta^2 \rho_s^2 - 1 + \rho_s^2 \mu^2 x^2] \phi_n^m = \hat{\Upsilon}_e^l \langle e^{-inq\theta} \phi_n \rangle_b \quad (13)$$

It is important to note that the above eigenmode equation has three distinct spatial scales, Δ , x_t , and x_i (see Fig.1). Here, $\Delta = \frac{1}{|k_\theta|s}$ is the separation between two adjacent mode rational surfaces for fixed n , $x_t = |\mu|^{-\frac{1}{2}}$ is the turning point of the mode, and $x_i = \frac{\omega L_n}{k_\theta v_i}$ is the Landau resonance point. The trapped electron response (the right side of Eq.(13)) varies on the scale Δ , the linear mode itself ϕ_n^m varies on the scale of x_t , and the spectrum $|\phi_n^m|^2$ varies on the scale x_i . For $k_\theta \rho_s \sim 1$, we observe that $\frac{\Delta}{x_t} \sim \sqrt{\frac{L_n}{L_s}}$, and $\frac{\Delta}{x_i} \sim \frac{L_n}{L_s} \sqrt{\frac{T_e}{T_i}}$. Each eigenmode, centered at a particular mode rational surface r_n , interacts with as many as $\frac{L_n}{L_s} (\gg 1)$ mode rational surfaces in it's neighborhood. In this case, the linear eigenmodes are said to be densely packed. A schematic picture of linear eigenmode structure with three spatial scale lengths Δ , x_t , and x_i is shown in Fig.1.

Equation (13) can be solved by treating the right side perturbatively. In lowest order, the solution is the Pearlstein-Berk outgoing wave function. For the most unstable mode (i.e. least shear damped), we have

$$\phi_n^m = \hat{\phi}_n^m e^{-i\mu \frac{x^2}{2}} \quad (14)$$

The outgoing wave boundary condition requires that μ should be an odd function of k_θ , i.e.

$$\mu = \frac{\omega_e^* L_n}{|\omega| L_s \rho_s^2} \quad (15)$$

The linear dispersion relation is determined by equation $\varepsilon(\vec{k}, \omega_{\vec{k}}) = 0$, where the linear dielectric function is $\varepsilon(\vec{k}, \omega) = \frac{\omega_e^*}{\omega} - k_\theta^2 \rho_s^2 - 1 - i\mu \rho_s^2$. The linear frequency and shear

damping rate are

$$\omega_{\vec{k}} = \frac{\omega_e^*}{1 + k_\theta^2 \rho_s^2} \quad (16)$$

$$\gamma^{sd} = -\frac{L_n}{L_s} |\omega_{\vec{k}}| \quad (17)$$

We next obtain the linear growth rate γ_e^l due to the trapped electron excitation. From perturbation theory, we have

$$\varepsilon(\vec{k}, \omega) = \frac{\int_{-\infty}^{\infty} dx \phi_n^m \hat{\Upsilon}_e^l \langle e^{-inq\theta} \phi_n \rangle_b}{\int_{-\infty}^{\infty} dx \phi_n^2} \quad (18)$$

where $\omega = \omega_{\vec{k}} + i\gamma^{sd} + i\gamma_e^l$. The detailed calculation of the spatial integrals in the above equation has been given in Ref.(2). Here, we only summarize some of the important results of the calculation. The spatial integral in the denominator of the above equation is easily evaluated as

$$\int_{-\infty}^{\infty} dx \phi_n^2 = \hat{\phi}_n^2 \sqrt{\frac{\pi}{i\mu}} \quad (19)$$

The spatial integral in the numerator, which involves the poloidal coupling effects, can be rewritten as

$$\begin{aligned} & \int_{-\infty}^{\infty} dx \phi_n^m \hat{\Upsilon}_e^l \langle e^{-inq\theta} \phi_n \rangle_b \\ &= \left(\frac{\epsilon}{2}\right)^{\frac{1}{2}} \left(1 - \frac{\omega_e^*}{\omega}\right) g_n \sum_{p=-\infty}^{\infty} \int_0^1 d\kappa^2 \int_{-\infty}^{\infty} dx \phi_n^m \phi_{m+p} \overline{e^{i(nq-m)\theta}} \langle e^{i(m+p-nq)\theta} \rangle_b \end{aligned} \quad (20)$$

As has been shown in Ref.(2), by keeping all p terms in Eq.(20), the integral is only a factor of $\frac{\pi}{2}$ times that obtained by keeping the p=0 term only. Hence, we can approximate Eq.(20) as

$$\begin{aligned} & \int_{-\infty}^{\infty} dx \phi_n^m \hat{\Upsilon}_e^l \langle e^{-inq\theta} \phi_n \rangle_b \\ &= \frac{\pi}{2} \left(\frac{\epsilon}{2}\right)^{\frac{1}{2}} \left(1 - \frac{\omega_e^*}{\omega}\right) g_n \int_0^1 d\kappa^2 \int_{-\infty}^{\infty} dx \phi_n^2 \overline{e^{i(nq-m)\theta}} \langle e^{i(m-nq)\theta} \rangle_b \end{aligned} \quad (21)$$

For small κ , we can approximate both $\overline{e^{i(nq-m)\theta}}$ and $\langle e^{i(m-nq)\theta} \rangle_b$ by $J_0(2\kappa \frac{x}{\Delta})$. Carrying out the κ and x integration in Eq.(21) by noting that $\int_0^\infty dt J_0^2(t) e^{-\beta t^2} \simeq \frac{1}{\pi} \ln \beta^{-\frac{1}{2}}$, we have

$$\int_{-\infty}^{\infty} dx \phi_n^l \hat{\Upsilon}_e^l \langle e^{-inq\theta} \phi_n \rangle_b \approx \left(\frac{\epsilon}{2}\right)^{\frac{1}{2}} \left(1 - \frac{\omega_e^*}{\omega}\right) g_n \hat{\phi}_n^2 \Delta \ln \frac{x_t}{\Delta} \quad (22)$$

Noting that $\varepsilon(\vec{k}, \omega) \approx i\gamma_e^l \frac{\partial}{\partial \omega} \varepsilon(\vec{k}, \omega_{\vec{k}})$, and $\frac{\partial}{\partial \omega} \varepsilon = -\frac{\omega_e^*}{\omega^2}$, the linear growth rate is obtained by substituting Eq.(19) and Eq.(22) into Eq.(18),

$$\frac{\gamma_e^l}{\omega_{\vec{k}}} = \left(\frac{\epsilon}{2}\right)^{\frac{1}{2}} \left(1 - \frac{\omega_{\vec{k}}}{\omega_e^*}\right) \Delta \ln\left(\frac{x_t}{\Delta}\right) \text{Im}(g_n \sqrt{\frac{i\mu}{\pi}}) \quad (23)$$

Eq.(23) shows that both $\text{Re}g_n$ and $\text{Im}g_n$ contribute to the linear growth rate, because $\sqrt{\frac{i\mu}{\pi}} = \sqrt{\frac{|\mu|}{2\pi}} [1 + i\text{sign}(k_\theta)]$ is complex (where $\text{sign}(k_\theta)$ is the sign function, equal to 1 for $k_\theta > 0$ and -1 for $k_\theta < 0$). This phenomenon is due to the fact that the eigenmode has outgoing wave structure and the trapped electron response and mode vary on different spatial scales. However, in the discussion of various trapped electron modes, the $\text{Re}g_n$ contribution to the linear growth rate can generally be neglected for the following two reasons. First, $\text{Re}g_n$ is smaller than $\text{Im}g_n$ in the dissipative regime. Second, the linear growth rate should be an even function of the poloidal wavenumber (k_θ). The contribution of $\text{Re}g_n$ to the linear growth rate, which is an odd function of k_θ , should be neglected even when $\text{Re}g_n$ is not necessarily smaller than $\text{Im}g_n$. By neglecting term associated with $\text{Re}g_n$ in Eq.(23), we finally have,

$$\frac{\gamma_e^l}{|\omega_{\vec{k}}|} = \frac{1}{2} \left(\frac{\epsilon}{\pi}\right)^{\frac{1}{2}} \left(1 - \frac{\omega_{\vec{k}}}{\omega_e^*}\right) \frac{\Delta}{x_t} \ln\left(\frac{x_t}{\Delta}\right) \text{Im}(g_n). \quad (24)$$

The above equation clearly indicates that due to the radial localization of trapped electron response, the linear growth rate of the mode is reduced by a factor of $\frac{\Delta}{x_t} \ln\left(\frac{x_t}{\Delta}\right) \propto \sqrt{\frac{L_n}{L_s}} < 1$. The instability source term $\text{Im}(g_n)$ in the above equation can be calculated from Eq.(11) in various collisionality regime. The results are:

1.) Collisionless Regime ($\omega > \omega_{De} > \nu_{eff}$)

$$\text{Im}(g_n) = 2\sqrt{\pi} \left(\frac{\omega}{\omega_{De}}\right)^{\frac{3}{2}} e^{-\frac{\omega}{\omega_{De}}} \quad (25a)$$

2.) Dissipative Regime ($\nu_{eff} > \omega > \omega_{De}$)

$$Im(g_n) = \frac{4}{\sqrt{\pi}} \frac{|\omega|}{\nu_{eff}} \quad (25b)$$

For typical tokamak parameters, it can be shown that the most unstable mode occurs at $k_{\theta} \rho_s \sim 1$, and the growth rate is smaller than the real frequency, i.e. $\frac{\gamma_e^l}{\omega} < 1$.

The important results of the linear analysis are summarized as follows. First, the linear eigenmode (slab-like) is characterized by three different spatial scale lengths Δ , x_t , and x_i ($\Delta < x_t < x_i$). Since the eigenmode spectrum extends to x_i , $\Delta(k_{\parallel} v_i) \sim \omega$ which implies that the wave-particle auto-correlation time is comparable to the wave period. This is in contrast to the shearless case where the wave-particle auto-correlation time is much longer than the wave period (i.e. $k_{\parallel} v_i \ll \omega$). Thus, nonlinear wave-particle interaction is much stronger in sheared slab than in a shearless system, where nonlinear wave-wave interaction is the dominant process. Second, the trapped electron mode is a short wavelength, strongly dispersive drift wave. Third, trapped electron response is radially localized to a narrow region $x \leq \Delta$ ($< x_t$) near the mode rational surface.

VI. Nonlinear Ion and Trapped Electron Response

In this section, weak turbulence theory is employed to calculate the nonlinear ion and trapped electron response. Since in the dissipative regime the trapped electron-mediated nonlinear interaction is negligible, we focus on the collisionless regime in the following analysis. The dissipative effect can be easily incorporated into the final result. In the weak turbulence theory, the nonlinear evolution of the mode occurs on a much slower time scale $\Delta\omega^{-1}$ than the linear mode oscillation ω^{-1} , where the turbulent decorrelation rate $\Delta\omega \sim \gamma_e^l \ll \omega$. The ions and electrons are primarily fluid-like, namely, they are not resonant with the drift wave. The turbulence spectrum can be decomposed into a sum of modes with frequency and mode structure described by linear theory. Nonlinearly, these modes can couple with each other in various ways.

By treating N_{ω}^i and N_{ω}^e as perturbations, we can solve Eqs.(3) and (6) perturbatively, namely, we expand h_{ω}^i , \hat{h}_{ω}^e , and ϕ_{ω} as $h_{\omega}^i = h_{\omega}^{i(1)} + h_{\omega}^{i(2)} + h_{\omega}^{i(3)} + \dots$, $\hat{h}_{\omega}^e = \hat{h}_{\omega}^{e(1)} + \hat{h}_{\omega}^{e(2)} + \hat{h}_{\omega}^{e(3)} + \dots$, and $\phi_{\omega} = \phi_{\omega}^{(1)} + \phi_{\omega}^{(2)} + \phi_{\omega}^{(3)} + \dots$. To the lowest order, we have the linear responses,

$$h_{\omega}^{i(1)} = \frac{e}{T_i} F_i \frac{\omega - \omega_i^*}{\omega - k_{\parallel} v_{\parallel}} J_0\left(\frac{k_{\perp} v_{\perp}}{\Omega_i}\right) \phi_{\omega}^{(1)} \quad (26a)$$

$$\hat{h}_{\omega}^{e(1)} = -\frac{e}{T_e} F_e \frac{\omega - \omega_e^*}{\omega - \omega_{de}} \langle e^{-inq\theta} \phi_{\omega}^{(1)} \rangle_b \quad (26b)$$

where $\phi_{\omega}^{(1)} = \phi_l^{(1)} \delta(\omega - \omega_{\bar{k}})$ is the linear eigenmode with $\omega_{\bar{k}}$ being the linear eigenfrequency.

In second order, we have a set of beat modes $h_{\omega''}^{i(2)}$, $\hat{h}_{\omega''}^{e(2)}$, and $\phi_{\omega''}^{(2)}$ which satisfy Eqs.(3) and (6), but are driven only by the direct interaction between the test mode (l, ω) and background mode (l', ω'),

$$h_{\omega''}^{i(2)} = \frac{e}{T_i} F_i \frac{\omega'' - \omega_i^{*''}}{\omega'' - k_{\parallel}'' v_{\parallel}} J_0\left(\frac{k_{\perp}'' v_{\perp}}{\Omega_i}\right) \phi_{\omega''}^{(2)} + \frac{i}{\omega'' - k_{\parallel}'' v_{\parallel}} S_{\omega''}^i \quad (27a)$$

$$\hat{h}_{\omega''}^{e(2)} = -\frac{e}{T_e} F_e \frac{\omega'' - \omega_e^{*''}}{\omega'' - \omega_{de}''} \langle e^{-in''q\theta} \phi_{\omega''}^{(2)} \rangle_b + \frac{i}{\omega'' - \omega_{de}''} S_{\omega''}^e \quad (27b)$$

where the driving terms $S_{\omega''}^i$ and $S_{\omega''}^e$ are given by,

$$S_{\omega''}^i = i \frac{c}{B} \left\{ k_{\theta} J_0\left(\frac{k_{\perp} v_{\perp}}{\Omega_i}\right) \phi_{\omega}^{(1)} \frac{\partial}{\partial r} h_{\omega'}^{i(1)} + k'_{\theta} J_0\left(\frac{k'_{\perp} v_{\perp}}{\Omega_i}\right) \phi_{\omega'}^{(1)} \frac{\partial}{\partial r} h_{\omega}^{i(1)} - k_{\theta} h_{\omega}^{i(1)} \frac{\partial}{\partial r} \left[J_0\left(\frac{k_{\perp} v_{\perp}}{\Omega_i}\right) \phi_{\omega'}^{(1)} \right] - k'_{\theta} h_{\omega'}^{i(1)} \frac{\partial}{\partial r} \left[J_0\left(\frac{k'_{\perp} v_{\perp}}{\Omega_i}\right) \phi_{\omega}^{(1)} \right] \right\} \quad (28a)$$

$$S_{\omega''}^e = i \frac{c}{B} \left\{ \frac{nq}{r} \langle e^{-inq\theta} \phi_{\omega}^{(1)} \rangle_b \frac{\partial}{\partial r} \hat{h}_{\omega'}^{e(1)} - \frac{nq}{r} \left(\frac{\partial}{\partial r} \langle e^{-in'q\theta} \phi_{\omega'}^{(1)} \rangle_b \right) \hat{h}_{\omega}^{e(1)} + \frac{n'q}{r} \langle e^{-in'q\theta} \phi_{\omega'}^{(1)} \rangle_b \frac{\partial}{\partial r} \hat{h}_{\omega}^{e(1)} - \frac{n'q}{r} \left(\frac{\partial}{\partial r} \langle e^{-inq\theta} \phi_{\omega}^{(1)} \rangle_b \right) \hat{h}_{\omega'}^{e(1)} \right\} \quad (28b)$$

The second order ion and electron density perturbation can be obtained from Eqs.(4) and (7) by integrating $h_{\omega''}^{i(2)}$ and $\hat{h}_{\omega''}^{e(2)}$ over velocity. To perform the velocity integration for ions, we neglect the resonance effect of the normal modes (l, ω) and (l', ω') in favor of the beat mode (l'', ω'') resonance, i.e. the ions are fluid-like relative to the normal modes $\omega \gg k_{\parallel} v_i$, and $\omega' \gg k'_{\parallel} v_i$. but are dissipative relative to the beat modes $\omega'' \leq k_{\parallel}'' v_i$. The results are

$$\delta n_{\omega''}^{i(2)} = \delta n_{\omega''}^{ii(2)} + \delta n_{\omega''}^{is(2)}$$

where $\delta n_{\omega''}^{il(2)}$ and $\delta n_{\omega''}^{is(2)}$ are the linear and nonlinear piece of the second order ion density response, and given by

$$\delta n_{\omega''}^{il(2)} = -\frac{e}{T_i} N \left[1 + \left(1 - \frac{\omega_i^{*''}}{\omega''} \right) \frac{\omega''}{|k_{\parallel}'' v_i|} Z \left(\frac{\omega''}{|k_{\parallel}'' v_i|} \right) \Gamma_0(b_i'') \right] \phi_{\omega''}^{(2)} \quad (29a)$$

$$\delta n_{\omega''}^{is(2)} = \frac{e}{T_e} N \frac{c}{B} \left(\frac{\omega_e^{*'}}{\omega'} - \frac{\omega_e^*}{\omega} \right) \frac{\langle J_0(k_{\perp} \rho_i) J_0(k'_{\perp} \rho_i) J_0(k''_{\perp} \rho_i) \rangle_{\perp}}{|k_{\parallel}'' v_i|} Z \left(\frac{\omega''}{|k_{\parallel}'' v_i|} \right) \\ (k_{\theta} \phi_{\omega}^{(1)} \frac{\partial}{\partial r} \phi_{\omega'}^{(1)} - k'_{\theta} \phi_{\omega'}^{(1)} \frac{\partial}{\partial r} \phi_{\omega}^{(1)}) \quad (29b)$$

where $b_i'' = \frac{1}{2} k_{\perp}''^2 \rho_i^2$, and

$$\langle J_0(k_{\perp} \rho_i) J_0(k'_{\perp} \rho_i) J_0(k''_{\perp} \rho_i) \rangle_{\perp} \equiv 2 \int_0^{\infty} x_{\perp} dx_{\perp} e^{-x_{\perp}^2} J_0(k_{\perp} \rho_i x_{\perp}) J_0(k'_{\perp} \rho_i x_{\perp}) J_0(k''_{\perp} \rho_i x_{\perp})$$

The velocity integrated trapped electron population can be obtained in a similar way. For most trapped electrons, we have $\omega \gg \omega_{de}$ and $\omega' \gg \omega'_{de}$, hence only a small number of high energy particles in the distribution tail can be resonant with the primary wave. However, since the beating mode frequency ω'' can become smaller than either ω or ω' , the bulk of the trapped electron distribution can be resonant with the beat wave. Thus, by retaining only the beat mode resonance effect in the trapped electron velocity integral, we have

$$\delta n_{\omega''}^{e(2)} = \delta n_{\omega''}^{el(2)} + \delta n_{\omega''}^{es(2)}$$

where $\delta n_{\omega''}^{el(2)}$, and $\delta n_{\omega''}^{es(2)}$ are given by

$$\delta n_{\omega''}^{el(2)} = \frac{e}{T_e} N (\phi_{\omega''}^{(2)} + \hat{\Upsilon}_e'' \langle e^{-in'' q \theta} \phi_{n''}^{(2)} \rangle_b) \quad (30a)$$

$$\hat{\Upsilon}_e'' \langle e^{-in'' q \theta} \phi_{n''}^{(2)} \rangle_b = 2 \left(\frac{\epsilon}{2} \right)^{\frac{1}{2}} g_{n''} \int_0^1 d\kappa^2 e^{i(n'' q - m'') \theta} \langle e^{-in'' q \theta} \phi_{n''}^{(2)} \rangle_b \quad (30b)$$

$$g_{n''} = \left(\frac{\omega_e^{*''}}{\omega''} - 1 \right) \frac{\omega''}{\omega_{De}''} \left[1 + \sqrt{\frac{\omega''}{\omega_{De}''}} Z \left(\sqrt{\frac{\omega''}{\omega_{De}''}} \right) \right]$$

and

$$\delta n_{\omega''}^{es(2)} = 2 \frac{e}{T_e} N \left(\frac{\epsilon}{2} \right)^{\frac{1}{2}} \frac{c}{B} \left(\frac{\omega_e^{*'}}{\omega'} - \frac{\omega_e^*}{\omega} \right) G_{n, n'}^e \int_0^1 d\kappa^2 e^{i(n'' q - m'') \theta}$$

$$\times \left[\frac{nq}{r} \langle e^{-inq\theta} \phi_{\omega}^{(1)} \rangle_b \frac{\partial}{\partial r} \langle e^{-in'q\theta} \phi_{\omega'}^{(1)} \rangle_b - \frac{n'q}{r} \langle e^{-in'q\theta} \phi_{\omega'}^{(1)} \rangle_b \frac{\partial}{\partial r} \langle e^{-inq\theta} \phi_{\omega}^{(1)} \rangle_b \right] \quad (31a)$$

$$G_{n,n'}^e = \frac{1}{\omega_{De}''} \left[1 + \sqrt{\frac{\omega''}{\omega_{De}''}} Z \left(\sqrt{\frac{\omega''}{\omega_{De}''}} \right) \right] \quad (31b)$$

By imposing the quasineutrality condition, we can obtain an equation that determines the second order potential perturbation $\phi_{\omega''}^{(2)}$,

$$\begin{aligned} & \left[1 + \tau + \tau \left(1 - \frac{\omega_i^{*''}}{\omega''} \right) \frac{\omega''}{|k_{\parallel}'' v_i|} \Gamma_0(b_i'') Z \left(\frac{\omega''}{|k_{\parallel}'' v_i|} \right) \right] \phi_{\omega''}^{(2)} + \hat{\Upsilon}^l \langle e^{-in''q\theta} \phi_{n''} \rangle_b \\ & = \hat{N}_{\omega''}^{i(s)} - \hat{N}_{\omega''}^{e(s)} \end{aligned} \quad (32)$$

where

$$\begin{aligned} \hat{N}_{\omega''}^{i(s)} &= \frac{T_e}{eN} \delta n_{\omega''}^{is(2)} \\ \hat{N}_{\omega''}^{e(s)} &= \frac{T_e}{eN} \delta n_{\omega''}^{es(2)} \end{aligned}$$

The left side of Eq.(32) is simply the linear dielectric for the beat mode (\vec{k}'', ω'') . The terms on the right side represent the drive by the direct interaction between the test mode (\vec{k}, ω) and the background mode (\vec{k}', ω') from both ion and trapped electron nonlinearity. Clearly, Eq.(32) is a very complicated, inhomogenous integral-differential equation which is not amenable to analytical solution. Nevertheless, some important properties of $\phi_{\omega''}^{(2)}$ relevant to our discussion can be obtained from simple physical considerations. First, $\phi_{\omega''}^{(2)}$ represents a process of nonlinear three wave resonance interaction (decay type interaction), i.e., $\phi_{\omega''}^{(2)} \propto \frac{1}{\varepsilon(\vec{k}'', \omega'')}$. The three wave resonance interaction is severely restricted by the dispersion of the primary wave. Second, in the presence of magnetic shear, the beat mode is intrinsically dissipative in nature (i.e., heavily Landau damped for $\omega + \omega' \leq k_{\parallel}'' v_i$). In order to see this, we note that the spectrum of the Pearlstein-Berk eigenmode extends to x_i such that $\Delta(k_{\parallel}' v_i) \sim \frac{k_{\perp}'}{L_s} \Delta x' v_i \sim \omega'$, hence the nonlinear ion Landau damping takes place when $\omega + \omega' \leq \Delta(k_{\parallel}'' v_i) \sim \omega'$. Therefore, in a sheared magnetic field, the range of frequency of the background mode which can interact with the test mode through ion Compton scattering is very broad. This is in contrast to the shearless case where the

condition that the ion is fluid-like $\omega \gg k_{\parallel} v_i$; implies that $\omega + \omega' < k_{\parallel} v_i \ll \omega'$ for beat mode interaction, i.e. without shear, the beat interaction is severely restricted. The strong dissipative character of the beat mode in a sheared magnetic field renders $\phi_{\omega''}^{(2)}$ significant only in a region of width x'' which is much narrower than the spatial width of the linear eigenmode spectrum x'_i (i.e. $x'' \ll x'_i$). As a consequence, the oft-referred-to cancellation of the shielding and bare scattering contributions to the order of $o(k_{\perp}^2 \rho_i^2)$, which occurs in the weak turbulence theory of shearless drift wave turbulence, does not occur in a sheared system.

Now, following standard procedures¹³, and making use of Eqs.(27a) and (27b), we have the third order perturbation in both h_i^i and \hat{h}_n^e ,

$$\begin{aligned}
h_i^{i(3)} = & \frac{c}{B} \frac{1}{\omega - k_{\parallel} v_{\parallel}} \sum_{\omega''} \left\{ -J_0\left(\frac{k'_{\perp} v_{\perp}}{\Omega_i}\right) \left[k_{\theta} \phi_{\omega''}^{(2)} \frac{\partial}{\partial r} h_{-\omega'}^{i(1)} + k'_{\theta} \frac{\partial}{\partial r} (\phi_{\omega''}^{(2)} h_{-\omega'}^{i(1)}) \right] \right. \\
& + \frac{e}{T_e} F_i J_0\left(\frac{k'_{\perp} v_{\perp}}{\Omega_i}\right) J_0\left(\frac{k'_{\perp} v_{\perp}}{\Omega_i}\right) \left[k_{\theta} \frac{\omega'' - \omega_i^{*''}}{\omega'' - k'_{\parallel} v_{\parallel}} \phi_{\omega''}^{(2)} \frac{\partial}{\partial r} \phi_{-\omega'}^{(1)} + k'_{\theta} \frac{\partial}{\partial r} \left(\frac{\omega'' - \omega_i^{*''}}{\omega'' - k'_{\parallel} v_{\parallel}} \phi_{\omega''}^{(2)} \phi_{-\omega'}^{(1)} \right) \right] \\
& \left. + J_0\left(\frac{k'_{\perp} v_{\perp}}{\Omega_i}\right) \left[\frac{i k_{\theta} S_{\omega''}^i}{\omega'' - k'_{\parallel} v_{\parallel}} \frac{\partial}{\partial r} \phi_{-\omega'}^{(1)} + \frac{\partial}{\partial r} \left(\frac{i k'_{\theta} S_{\omega''}^i}{\omega'' - k'_{\parallel} v_{\parallel}} \phi_{-\omega'}^{(1)} \right) \right] \right\} \quad (33a)
\end{aligned}$$

and

$$\begin{aligned}
\hat{h}_n^{e(3)} = & \frac{c}{B} \frac{1}{\omega - \omega_{de}} \sum_{\omega''} \left\{ -\frac{nq}{r} \langle e^{-in''q\theta} \phi_{\omega''}^{(2)} \rangle_b \frac{\partial}{\partial r} \hat{h}_{-\omega'}^{e(1)} - \frac{n'q}{r} \frac{\partial}{\partial r} (\langle e^{-in''q\theta} \phi_{\omega''}^{(2)} \rangle_b \hat{h}_{-\omega'}^{e(1)}) \right. \\
& - \frac{e}{T_e} F_e \frac{\omega'' - \omega_e^{*''}}{\omega'' - \omega_{de}''} \left[\frac{nq}{r} \langle e^{-in''q\theta} \phi_{\omega''}^{(2)} \rangle_b \frac{\partial}{\partial r} \langle e^{in'q\theta} \phi_{-\omega'}^{(1)} \rangle_b + \frac{n'q}{r} \frac{\partial}{\partial r} (\langle e^{-in''q\theta} \phi_{\omega''}^{(2)} \rangle_b \langle e^{in'q\theta} \phi_{-\omega'}^{(1)} \rangle_b) \right] \\
& \left. + \frac{i}{\omega'' - \omega_{de}''} \left[\frac{nq}{r} S_{\omega''}^e \frac{\partial}{\partial r} \langle e^{in'q\theta} \phi_{-\omega'}^{(1)} \rangle_b + \frac{n'q}{r} \frac{\partial}{\partial r} (S_{\omega''}^e \langle e^{in'q\theta} \phi_{-\omega'}^{(1)} \rangle_b) \right] \right\} \quad (33b)
\end{aligned}$$

On the right side of the above equations, the first two terms that involve $\phi_{\omega''}^{(2)}$ or $\phi_{\omega''}^{(2)}$ represent nonlinear three wave resonant interaction effects. The last two terms that involve the resonance factor $\frac{1}{\omega'' - k'_{\parallel} v_{\parallel}}$ or $\frac{1}{\omega'' - \omega_{de}''}$ represent the effect of scattering of waves by bare particles, namely, the ion Compton scattering and trapped electron Compton scattering (nonlinear trapped electron-wave interaction). The second two terms that involve both

$\phi_{\omega''}^{(2)}$, and the resonance factor represent the effect of scattering of waves by the shielding or polarization cloud generated by a moving charged particle. For slab-like trapped electron drift modes, the three wave resonance interaction is irrelevant since the most unstable modes are short wavelength dispersive waves ($k_{\theta\rho_s} \approx 1$) so that the beat mode is not resonant. The effect of the scattering of waves by the shielding cloud is weak because the second order potential perturbation $\phi_{\omega''}^{(2)}$ is radially localized to a region which is much more narrower than the linear mode width ($x_i'' \ll x_i'$). Therefore, in a sheared magnetic field, the dominant nonlinear process is the bare particle induced wave scattering. In the following discussion, terms associated with $\phi_{\omega''}^{(2)}$ will be neglected. By making use of Eqs.(28a) and (28b), and keeping only the beat-mode-particle resonance effect, we have the third order ion and trapped electron response,

$$\hat{h}_n^{i(3)} = -k_{\theta}^2 \mu_{\theta\theta}^i J_0\left(\frac{k_{\perp} v_{\perp}}{\Omega_i}\right) \phi_n^m + \mu_{rr}^i J_0\left(\frac{k_{\perp} v_{\perp}}{\Omega_i}\right) \frac{\partial^2}{\partial r^2} \phi_n^m \quad (34a)$$

$$\hat{h}_n^{e(3)} = -\left(\frac{nq}{r}\right)^2 \mu_{\theta\theta}^e \langle e^{-inq\theta} \phi_n \rangle_b + \mu_{rr}^e \frac{\partial^2}{\partial r^2} \langle e^{-inq\theta} \phi_n \rangle_b \quad (34b)$$

where the spectrum dependent quantities are

$$\mu_{\theta\theta}^i = \left(\frac{c}{B}\right)^2 \frac{1}{\omega} \sum_{\frac{m'}{n'}} R_{m''} J_0^2\left(\frac{k'_{\perp} v_{\perp}}{\Omega_i}\right) \left| \frac{\partial}{\partial r} \phi_{n'}^m \right|^2 \frac{e}{T_i} F_i\left(\frac{\omega_i^*}{\omega} - \frac{\omega_i^{*'}}{\omega'}\right)$$

$$\mu_{rr}^i = \left(\frac{c}{B}\right)^2 \frac{1}{\omega} \sum_{\frac{m'}{n'}} R_{m''} k_{\theta}^2 J_0^2\left(\frac{k'_{\perp} v_{\perp}}{\Omega_i}\right) \left| \phi_{n'}^m \right|^2 \frac{e}{T_i} F_i\left(\frac{\omega_i^*}{\omega} - \frac{\omega_i^{*'}}{\omega'}\right)$$

$$R_{m''} = \frac{1}{\omega'' - k_{\parallel}'' v_{\parallel}}$$

$$\mu_{\theta\theta}^e = \left(\frac{c}{B}\right)^2 \frac{1}{\omega} \sum_{n'} R_{n''} \left| \frac{\partial}{\partial r} \langle e^{-in'q\theta} \phi_{n'} \rangle_b \right|^2 \frac{e}{T_e} F_e\left(\frac{\omega_e^{*'}}{\omega'} - \frac{\omega_e^*}{\omega}\right)$$

$$\mu_{rr}^e = \left(\frac{c}{B}\right)^2 \frac{1}{\omega} \sum_{n'} R_{n''} \left(\frac{n'q}{r}\right)^2 \left| \langle e^{-in'q\theta} \phi_{n'} \rangle_b \right|^2 \frac{e}{T_e} F_e\left(\frac{\omega_e^{*'}}{\omega'} - \frac{\omega_e^*}{\omega}\right)$$

$$R_{n''} = \frac{1}{\omega'' - \omega_{de}''}$$

In arriving at the above results, the fact that the linear modes are densely packed has been utilized so that only terms with even parity in x' are retained, while terms with odd

parity in x' like $\psi_{-\omega'}^{(1)} \frac{\partial}{\partial r} \psi_{\omega'}^{(1)}$ and $\langle e^{in'q\theta} \phi_{-\omega'}^{(1)} \rangle_b \frac{\partial}{\partial r} \langle e^{-in'q\theta} \phi_{\omega'}^{(1)} \rangle_b$ vanish. The superfluous subscripts ω, ω' on all the fluctuating quantities have been dropped, since they are related to the wavenumbers n and n' through the linear dispersion relation $\omega = \omega_{\vec{k}}$, and $\omega' = \omega_{\vec{k}'}$. Without any confusion, $\phi_n^{(1)}$, and $\phi_{\omega'}^{(1)}$ have been replaced by ϕ_n and $\phi_{n'}$ to represent the linear eigenmode. The ion density response up to third order is then given by

$$\begin{aligned} \delta n_m^i &= -\frac{e}{T_e} N \phi_n^m + \int d^3 \vec{v} J_0 \left(\frac{k_{\perp} v_{\perp}}{\Omega_i} \right) (h_n^{i(1)} + h_n^{i(3)}) \\ &= \delta n_m^{i(1)} + \delta n_m^{i(3)} \end{aligned} \quad (35)$$

where $\delta n_m^{i(1)}$ is the linear ion density response given by Eq.(12), $\delta n_m^{i(3)}$ is the third order ion density response and can be obtained by integrating Eq.(43) over velocity space,

$$\delta n_m^{i(3)} = \frac{e}{T_e} N [-k_{\theta}^2 D_{\theta\theta}^i + D_{rr}^i \frac{\partial^2}{\partial r^2}] \phi_n^m \quad (36)$$

where

$$D_{\theta\theta}^i = \frac{1}{\omega} \left(\frac{c}{B} \right)^2 \sum_{n'} \left| \frac{\partial}{\partial r} \phi_{n'}^m \right|^2 \left(\frac{\omega_e^*}{\omega} - \frac{\omega_e'^*}{\omega'} \right) G_{mn, m'n'}^i \quad (37a)$$

$$D_{rr}^i = \frac{1}{\omega} \left(\frac{c}{B} \right)^2 \sum_{n'} k_{\theta}^{\prime 2} |\phi_{n'}^m|^2 \left(\frac{\omega_e^*}{\omega} - \frac{\omega_e'^*}{\omega'} \right) G_{mn, m'n'}^i. \quad (37b)$$

The interaction kernel $G_{mn, m'n'}^i$ is

$$G_{mn, m'n'}^i = \langle J_0^2(k_{\perp} \rho_i) J_0^2(k'_{\perp} \rho_i) \rangle_{\perp} \frac{1}{|k''_{\parallel} v_i|} Z \left(\frac{\omega''}{|k''_{\parallel} v_i|} \right) \quad (38)$$

where

$$\langle J_0^2(k_{\perp} \rho_i) J_0^2(k'_{\perp} \rho_i) \rangle_{\perp} = 2 \int_0^{\infty} x_{\perp} dx_{\perp} e^{-x_{\perp}^2} J_0^2(k_{\perp} \rho_i x_{\perp}) J_0^2(k'_{\perp} \rho_i x_{\perp}).$$

The electron density response up to third order is given by

$$\begin{aligned} \delta n_m^e &= \frac{e}{T_e} N \phi_n^m + \int_{-\pi}^{\pi} \frac{d\theta}{2\pi} e^{i(nq-m)\theta} \int_t d^3 \vec{v} (\hat{h}_n^{e(1)} + \hat{h}_n^{e(3)}) \\ &= \delta n_m^{e(1)} + \delta n_m^{e(3)} \end{aligned} \quad (39)$$

where $\delta n_m^{e(1)}$ is the linear electron response, given by Eqs.(10a) and (10b), $\delta n_m^{e(3)}$ is the nonlinear trapped electron response and can be obtained by using Eq.(34b),

$$\delta n_m^{e(3)} = \frac{e}{T_e} N \hat{\Upsilon}_e^{nl} \langle e^{-inq\theta} \phi_n \rangle_b \quad (40a)$$

$$\hat{\Upsilon}_e^{nl} \langle e^{-inq\theta} \phi_n \rangle_b = \left(\frac{e}{2}\right)^{\frac{1}{2}} \int_0^1 d\kappa^2 e^{i(nq-m)\theta} \left[-\left(\frac{nq}{r}\right)^2 D_{\theta\theta}^e + D_{rr}^e \frac{\partial^2}{\partial r^2} \right] \langle e^{-inq\theta} \phi_n \rangle_b \quad (40b)$$

with

$$D_{\theta\theta}^e = \frac{2}{\omega} \left(\frac{c}{B}\right)^2 \sum_{n'} \left| \frac{\partial}{\partial r} \langle e^{-in'q\theta} \phi_{n'} \rangle_b \right|^2 \left(\frac{\omega_e^*}{\omega} - \frac{\omega_e^{*'}}{\omega'} \right) G_{n,n'}^e \quad (41a)$$

$$D_{rr}^e = \frac{2}{\omega} \left(\frac{c}{B}\right)^2 \sum_{n'} \left(\frac{n'q}{r}\right)^2 \left| \langle e^{-in'q\theta} \phi_{n'} \rangle_b \right|^2 \left(\frac{\omega_e^*}{\omega} - \frac{\omega_e^{*'}}{\omega'} \right) G_{n,n'}^e \quad (41b)$$

V. Wave Kinetic Equation for Trapped Electron Mode Turbulence

In this section, we derive a wave kinetic equation which describes the nonlinear evolution of the fluctuation spectrum using the previously derived nonlinear responses. By imposing the quasineutrality condition $\delta n_m^e = \delta n_m^i$ for the nonlinear responses, we obtain a nonlinear eigenmode equation

$$\begin{aligned} & \left\{ \rho_s^2 \frac{\partial^2}{\partial r^2} + \frac{\omega_e^*}{\omega} - k_\theta^2 \rho_s^2 - 1 + \mu^2 \rho_s^2 x^2 \right\} \phi_m \\ & = (\hat{\Upsilon}_e^l + \hat{\Upsilon}_e^{nl}) \langle e^{-inq\theta} \phi_n \rangle_b + (k_\theta^2 D_{\theta\theta}^i - D_{rr}^i \frac{\partial^2}{\partial r^2}) \phi_m \end{aligned} \quad (42)$$

To solve this equation, techniques in solving the linear eigenmode equation are again utilized, i.e. we treat the terms on the right side of Eq.(42) as perturbations. This is possible because in the weak turbulence theory, the nonlinear interaction is at most comparable to the linear growth rate. In lowest order, we have the outgoing wave solution for the most unstable (least shear damped) mode,

$$\phi_m^{(0)} = \hat{\phi}_m e^{-\frac{i\mu x^2}{2}}$$

the corresponding real frequency,

$$\omega_{\vec{k}} = \frac{\omega_e^*}{1 + k_\theta^2 \rho_s^2}$$

and the shear damping rate

$$\gamma^{sd} = -\frac{L_n}{L_s} |\omega_{\vec{k}}|$$

To the next order, from perturbation theory we have,

$$\varepsilon(\vec{k}, \omega) \int_{-\infty}^{\infty} dx (\phi_n^{(0)})^2 = I_e^l + I_e^{nl} + I_i^{nl} \quad (43)$$

where $\omega = \omega_{\vec{k}} + i\gamma$, and I_e^l , I_e^{nl} and I_i^{nl} are defined by the following integrals,

$$I_e^l = \int_{-\infty}^{\infty} dx \phi_n^{(0)} \hat{\Upsilon}_e^l \langle e^{-inq\theta} \phi_n^{(0)} \rangle_b \quad (44a)$$

$$I_e^{nl} = \int_{-\infty}^{\infty} dx \phi_n^{(0)} \hat{\Upsilon}_e^{nl} \langle e^{-inq\theta} \phi_n^{(0)} \rangle_b \quad (44b)$$

$$I_i^{nl} = \int_{-\infty}^{\infty} dx \{ k_\theta^2 D_{\theta\theta}^{i(0)} (\phi_n^{(0)})^2 + D_{rr}^{i(0)} \left(\frac{\partial}{\partial r} \phi_n^{(0)} \right)^2 \} \quad (44c)$$

It is interesting to note that the above integrals involve $\phi_n^{(0)2}$ rather than $|\phi_n^{(0)}|^2$. Therefore, it is expected that the principal contribution to the integrals is from the region $x < x_t$ where the mode is non-oscillatory. Outside this region, rapid cancelation in the integration occurs because of the fast oscillation character of $\phi_n^{(0)2}$ for $x > x_t$. Physically, this can be interpreted as that only the energy input or outflow in region $x < x_t$ is relevant to the growth or damping of the mode. The first integral I_e^l has been evaluated in Sec.III (Eq.(22)). By noting that for $x_t > \Delta$, we have $\frac{\partial}{\partial r} \langle e^{-inq\theta} \phi_n \rangle_b \simeq \frac{1}{\Delta} \langle e^{-inq\theta} \phi_n \rangle_b$, I_e^{nl} can be evaluated in the same way. The result is

$$I_e^{nl} \simeq -\left(\frac{\varepsilon}{2}\right)^{\frac{1}{2}} \int_0^1 d\kappa [k_\theta^2 D_{\theta\theta}^e + \left(\frac{2\kappa}{\Delta}\right)^2 D_{rr}^e] \Delta \ln\left(\frac{2\kappa x_t}{\Delta}\right) \hat{\phi}_n^2 \quad (45)$$

For I_i^{nl} , we note that the spectrum dependent quantities D_{rr}^i and $D_{\theta\theta}^i$ varies slowly with x on the spatial scale of x_i , because they involve $|\phi_{n'}^0|^2$ rather than $\phi_{n'}^0{}^2$. Therefore, in evaluating the integral I_i^{nl} , $D_{rr}^i(x)$ and $D_{\theta\theta}^i(x)$ can be replaced by $D_{rr}^i(0)$ and $D_{\theta\theta}^i(0)$. The integral I_i^{nl} can then be easily evaluated,

$$I_i^{nl} = [k_\theta^2 D_{\theta\theta}^{i(0)} - \frac{i}{2} \mu D_{rr}^{i(0)}] \sqrt{\frac{\pi}{i\mu}} \hat{\phi}_n^2 \quad (46)$$

Noting Eq.(19), we multiply Eq.(43) on both side by $\sqrt{\frac{i\mu}{\pi}}$. Replacing $\hat{\phi}_n^2$ by $|\hat{\phi}_n|^2$, and then taking the imaginary part of the equation, we obtain,

$$\begin{aligned}
Im\varepsilon(\vec{k}, \omega)|\hat{\phi}_n|^2 &= \left(\frac{\varepsilon}{2}\right)^{\frac{1}{2}} \left(1 - \frac{\omega_e^*}{\omega}\right) \Delta \ln \frac{x_t}{\Delta} |\hat{\phi}_n|^2 Im(g_n \sqrt{\frac{i\mu}{\pi}}) \\
&\quad - \left(\frac{\varepsilon}{2}\right)^{\frac{1}{2}} \int_0^1 d\kappa [k_\theta^2 Im(D_{\theta\theta}^e \sqrt{\frac{i\mu}{\pi}}) + \left(\frac{2\kappa}{\Delta}\right)^2 Im(D_{rr}^e \sqrt{\frac{i\mu}{\pi}})] \Delta \ln\left(\frac{2\kappa x_t}{\Delta}\right) |\hat{\phi}_n|^2 \\
&\quad + [k_\theta^2 Im(D_{\theta\theta}^{i(0)}) - \frac{1}{2} \mu Re(D_{rr}^{i(0)})] |\hat{\phi}_n|^2
\end{aligned} \tag{47}$$

For the same reasons as we have discussed in Sec.III the nonresonant terms associated with $Re(g_n)$, $Re(D_{\theta\theta}^e)$, $Re(D_{rr}^e)$ and $Re(D_{rr}^i)$ on the right side of the above equation can be neglected. The further reason for neglecting $Re D_{rr}^i$ is that $k_\theta^2 > \mu$ for the most unstable mode. By noting that $Im\varepsilon(\vec{k}, \omega) \approx \frac{\partial\varepsilon}{\partial\omega}(\gamma - \gamma^{sd})$, and replacing γ by $\frac{1}{2} \frac{\partial}{\partial t}$, we obtain the wave kinetic equation,

$$\frac{\partial}{\partial t} |\phi_n|^2 = 2(\gamma_e^l + \gamma^{sd} + \gamma_e^{nl} + \gamma_i^{nl}) |\phi_n|^2 \tag{48}$$

In the above equation, γ_e^l and γ^{sd} are the linear growth rate and the shear damping rate given by Eq.(24) and Eq.(17), respectively, γ_i^{nl} and γ_e^{nl} are the nonlinear transfer rates due to ion Compton scattering and trapped electron Compton scattering. Using Eq.(47) and $\frac{\partial\varepsilon}{\partial\omega} = -\frac{\omega_e^*}{\omega^2}$, we have,

$$\frac{\gamma_i^{nl}}{|\omega_{\vec{k}}|} = -\frac{\omega_{\vec{k}}}{|\omega_e^*|} k_\theta^2 Im D_{\theta\theta}^i \tag{49}$$

$$\frac{\gamma_e^{nl}}{|\omega_{\vec{k}}|} = \frac{1}{2} \frac{\omega_{\vec{k}}}{|\omega_e^*|} \left(\frac{\varepsilon}{\pi}\right)^{\frac{1}{2}} \int_0^1 d\kappa \frac{\Delta}{x_t} \ln\left(\frac{2\kappa x_t}{\Delta}\right) [k_\theta^2 Im D_{\theta\theta}^e + \left(\frac{2\kappa}{\Delta}\right)^2 Im D_{rr}^e] \tag{50}$$

where $D_{\theta\theta}^i$ is evaluated at $x = 0$.

VI. Nonlinear Wave-Particle Interaction in a Sheared Magnetic Field

In this section, nonlinear wave-particle interaction, namely, ion Compton scattering and trapped electron Compton scattering, in a sheared magnetic field are discussed. The effect of slab-like eigenmode structure on the nonlinear wave-particle interaction is

explored. Specifically, we find that ion Compton scattering is enhanced while trapped electron Compton scattering is weakened. Therefore, ion Compton scattering rather than trapped electron Compton scattering is the dominant nonlinear saturation mechanism of trapped electron mode turbulence in a sheared magnetic field.

From Eqs.(49) and (50) and noting Eqs.(37a), (41a), and (41b), the nonlinear transfer rates due to ion Compton scattering and trapped electron Compton scattering can be rewritten as

$$\gamma_i^{nl} = \frac{\omega_{\bar{k}}}{\omega_e^*} k_\theta^2 \left(\frac{c}{B}\right)^2 \sum_{m'} \left| \frac{\partial}{\partial r} \phi_{m'} \right|^2 (k_\theta'^2 - k_\theta^2) \rho_s^2 \text{Im} G_{mn, m'n'}^i \quad (51)$$

$$\begin{aligned} \gamma_e^{nl} = & \frac{\omega_{\bar{k}}}{\omega_e^*} \left(\frac{e}{\pi}\right)^{\frac{1}{2}} \left(\frac{c}{B}\right)^2 \int_0^1 d\kappa \frac{\Delta}{x_t} \ln\left(\frac{x_t}{\Delta}\right) \sum_{n'} (k_\theta'^2 - k_\theta^2) \rho_s^2 \\ & \times \left\{ k_\theta^2 \left| \frac{\partial}{\partial r} \langle e^{-in'q\theta} \phi_{n'} \rangle_b \right|^2 + \left(\frac{2\kappa}{\Delta}\right)^2 \left| \langle e^{-in'q\theta} \phi_{n'} \rangle_b \right|^2 \right\} \text{Im} G_{n, n'}^e \end{aligned} \quad (52)$$

From Eq.(38), the interaction kernel for ion Compton scattering is given by

$$\text{Im} G_{mm', nn'}^i = \langle J_0^2(k_\perp \rho_i) J_0^2(k'_\perp \rho_i) \rangle_\perp \frac{\sqrt{\pi}}{|k'_\parallel v_i|} e^{-\left(\frac{\omega'}{k'_\parallel v_i}\right)^2} \quad (53)$$

For trapped electron Compton scattering, we note that $\omega \gg \omega_{de}$ and $\omega' \gg \omega'_{de}$, so that $G_{n, n'}^e$ in Eq.(31b) can be approximated by $G_{n, n'}^e \approx -\frac{1}{2\omega'}$, hence,

$$\text{Im} G_{n, n'}^e = \frac{\pi}{2} \delta(\omega + \omega') \quad (54)$$

Now, we discuss the physical implications of Eqs.(51)-(54). First, from the direct observation of Eqs.(51)-(54), we note that for $k_\theta < k'_\theta$, $\gamma_i^{nl} > 0$ but $\gamma_e^{nl} < 0$, i.e. a long wavelength mode is nonlinearly excited by ion Compton scattering but nonlinearly damped by trapped electron Compton scattering; for $k_\theta > k'_\theta$, $\gamma_i^{nl} < 0$ but $\gamma_e^{nl} > 0$, alternatively a short wavelength mode is nonlinearly damped by ion Compton scattering but nonlinearly excited by trapped electron Compton scattering. Therefore, we have two competitive nonlinear transfer processes: ion Compton scattering transfers wave energy from short to long wavelengths while trapped electron Compton scattering transfers wave

energy from long to short wavelengths. Second, we note that the interaction kernel for ion Compton scattering has a broad band spectrum with width $\Delta\omega'' \simeq k'_{\parallel}(x)v_i$. Since the slab-like eigenmode spectrum $|\phi_n|^2$ can extend to x_i , the width of the interaction kernel is $\Delta\omega'' \sim k'_{\parallel}(x'_i)v_i \sim \omega'$, which indicates any beat mode with frequency ω'' in the range $\Delta\omega'' \sim \omega'$ can be very easily coupled with the ions. The ion Compton scattering process is therefore considerably enhanced. This frequency spread or “resonance broadening” is caused by the magnetic shear induced Doppler shift. In order to see this, it is instructive to note that in the shearless case, we have $\omega' \gg k'_{\parallel}v_i$. Thus the interaction kernel in the shearless case can be obtained by taking the limit $k'_{\parallel}v_i \rightarrow 0$,

$$\lim_{k'_{\parallel}v_i \rightarrow 0} \text{Im}G_{mm',nn'}^i = \langle J_0^2(k_{\perp}\rho_i)J_0^2(k'_{\perp}\rho_i) \rangle_{\perp} \pi\delta(\omega'')$$

namely, the ion Compton scattering is (severely) restricted to be local in frequency. As a consequence of the Doppler ‘resonance broadening’, the ion Compton scattering process in a sheared magnetic field is fundamentally different from that in a shearless case. This is because: 1) local energy transfer (with comparable wave numbers $k'_{\theta} \sim k_{\theta}$) which is absent in the shearless case is now very robust in the long wavelength part of the spectrum. ii.) ion Compton scattering is no longer an adiabatic process, namely, significant amount of wave energy is transferred directly to the ions (nonlinear ion heating). Third, due to the radial localization of trapped electron response, trapped electron Compton scattering is restricted to a very narrow layer of width Δ near mode rational surface. Hence, the intensity of the scattering is significantly reduced. This is apparent from Eq.(52) that $\gamma_e^{n'l} \propto \frac{\Delta}{x_t} \ln \frac{x_t}{\Delta}$ and the fact that $|(e^{-in'q\theta} \phi_{n'})_b|^2$ is much smaller than $|\phi_{n'}|^2$.

We now evaluate the nonlinear couplings (i.e., the summations) in Eq.(51) and (52). Since the linear modes are densely packed, we can treat both m' and n' as continuous variables, so that the summations in both Eq.(51) and Eq.(52) can be converted into integrals according to $\sum_{m'} = \int dn' \int dm'$. Noting that $k'_{\theta} = \frac{n'q}{r}$ and $m' = n'q(r_{\frac{m'}{n'}})$, we

have $dn' = \frac{r}{q} dk'_\theta$, and $dm' = \frac{1}{\Delta'} dr_{m'}$ for fixed n' , hence,

$$\sum_{\frac{m'}{n'}} = \frac{r}{q} \int \frac{dk'_\theta}{\Delta'} \int dr_{m'}. \quad (55)$$

In order to complete the integral, an explicit form of the spatial structure of the spectrum function $|\phi_{\frac{m}{n}}|^2$ is required. The integral is only sensitive to the spatial width of the spectrum w' rather than to the exact form of its spatial structure. By noting that $|\phi_{\frac{m}{n}}|^2$ changes slowly for $x' < w'$, but decays rapidly for $x' > w'$, we can approximate $|\phi_{\frac{m}{n}}|^2$ as

$$|\phi_{\frac{m}{n}}|^2 = |\phi(k_\theta)|^2 \theta(|x'| - w') \quad (56)$$

where $\theta(|x'| - w')$ is the heavyside step function.

a. Nonlinear Transfer Rate Due to Ion Compton Scattering

In evaluating $\gamma_i^{n'}$, noting that in the limit $T_e \gg T_i$, $\langle J_0^2(k_\perp \rho_i) J_0^2(k'_\perp \rho_i) \rangle_\perp$ can be approximated by 1. From Eqs.(51), and (53), and noting that $|\frac{\partial}{\partial r} \phi_{\frac{m'}{n'}}|^2 \approx \mu'^2 x'^2 |\phi|^2(k'_\theta) \theta(|x'| - w')$, $k'_\parallel v_i = \frac{\omega' x'}{x'_i}$, $x'_i = \frac{\omega' L_n}{k'_\theta v_i}$, the nonlinear transfer rate for ion Compton scattering can be rewritten as

$$\begin{aligned} \frac{\gamma_i^{n'}}{|\omega|} &= \left(\frac{c}{B}\right)^2 \frac{k_\theta^2}{|\omega_e^*|} \frac{r}{q} \int \frac{dk'_\theta}{\Delta'} |\phi|^2(k'_\theta) (k_\theta'^2 - k_\theta^2) \rho_s^2 \\ &\times \int_{r-w'}^{r+w'} dr_{m'} \mu'^2 x'^2 \frac{\sqrt{\pi} x'_i}{|\omega' x'|} \exp\left\{-\left(\frac{\omega' x'_i}{\omega' x'}\right)^2\right\} \end{aligned} \quad (57)$$

It is important to note that in a sheared magnetic field the radial wavenumber k'_r is a function of x' , i.e., $k'_r = -\mu' x'$, which implies that nonlinear ion coupling is stronger for larger x' . The fact that the slab-like eigenmode spectrum extends to x'_i renders $|k'_r| \sim |\mu' x'_i| \sim \sqrt{\frac{L_n}{L_n}} x_i^{-1} > x_i^{-1}$. Hence, due to the strong nonlinear coupling, ion Compton scattering is expected to be much more robust in a sheared magnetic field. Thus, saturation at levels below the conventionally quoted mixing length estimate of $\frac{\bar{n}}{n_0} \sim \frac{x_i}{L_n}$ appears likely. Note also that since $k'_r \rho_i \leq 1$, the replacing of $\langle J_0^2(k_\perp \rho_i) J_0^2(k'_\perp \rho_i) \rangle_\perp$ by 1 in the weak

turbulence theory constitutes only a slight quantitative error. Changing variable from $r_{n'}$ to $x' = r - r_{n'}$ and carrying out the x' integration in the above equation, we have

$$\frac{\gamma_i^{nl}}{|\omega|} = \sqrt{\pi} \frac{T_e}{T_i} \left(\frac{c}{B}\right)^2 \frac{k_\theta^2}{|\omega_e^*|} \frac{r}{q} \int \frac{dk'_\theta}{|\omega'|} |\phi|^2(k'_\theta) (k_\theta'^2 - k_\theta^2) \frac{w'}{x'_i} \frac{2w'}{\Delta'} E_2\left[\left(\frac{\omega'' x'_i}{\omega' w'}\right)^2\right] \quad (58)$$

where $E_2(x) = \int_1^\infty dy y^{-2} \exp\{-xy\}$ is the exponential function. $E_2\left[\left(\frac{\omega'' x'_i}{\omega' w'}\right)^2\right]$ is sharply peaked around ω'' with a frequency spread $\Delta\omega'' \sim \omega' \left(\frac{w'}{x'_i}\right)$. Noting that

$$\frac{\omega''}{\omega'} = \frac{(k'_\theta - k_\theta)(1 - k_\theta k'_\theta \rho_s^2)}{k'_\theta(1 + k_\theta^2)(1 + k_\theta'^2)},$$

small ω'' can be achieved either around $k'_\theta \sim k_\theta^+ = k_\theta$ (local interaction) or around $k'_\theta \sim k_\theta^- = \frac{1}{k_\theta \rho_s^2}$ (nonlocal interaction) which is depicted in Fig.2. The fact that $E_2\left[\left(\frac{\omega'' x'_i}{\omega' w'}\right)^2\right]$ is sharply peaked around k_θ^+ and k_θ^- allows us to simplify the expression for γ_i^{nl} considerably, namely, to convert the integral operator in Eq.(58) into a differential operator. In order to do this, let's expand $|\phi|^2(k'_\theta)$ in a Taylor series around $k_\theta^j = k_\theta^+, k_\theta^-$, i.e.

$$|\phi|^2(k'_\theta) = |\phi|^2(k_\theta^j) + \frac{\partial}{\partial k_\theta^j} |\phi|^2(k_\theta^j) (k'_\theta - k_\theta^j) + \dots \quad (59)$$

This expansion is valid only when

$$\frac{\partial}{\partial k_\theta} |\phi|^2(k_\theta^j) (k'_\theta - k_\theta^j) < |\phi|^2(k_\theta^j)$$

Taking $k'_\theta - k_\theta^j \sim \overline{\Delta k_\theta}_{E_2}$ and $\frac{1}{|\phi|^2(k_\theta^j)} \frac{\partial}{\partial k_\theta} |\phi|^2(k_\theta^j) = \frac{1}{\overline{\Delta k_\theta}_\phi}$, where $\overline{\Delta k_\theta}_{E_2}$ is the spectrum width of the interaction kernel $E_2\left[\left(\frac{\omega'' x'_i}{\omega' w'}\right)^2\right]$, and $\overline{\Delta k_\theta}_\phi$ is the spectrum width of $|\phi|^2(k_\theta)$, the condition above can be rewritten as

$$\overline{\Delta k_\theta}_{E_2} < \overline{\Delta k_\theta}_\phi$$

namely, the spectrum width of the interaction kernel must be narrower than the width of the fluctuation spectrum.

To simplify Eq.(58), we first calculate the local interaction contribution to γ_i^{nl} . We define a new variable $k_\theta'' = k'_\theta - k_\theta$. Near k_θ , we have $\frac{\omega'' x'_i}{\omega' w'} \simeq \alpha^+ k_\theta''$, where $\alpha^+ =$

$|\frac{1-k_\theta^2\rho_s^2}{k_\theta(1+k_\theta^2\rho_s^2)}|\frac{x_i'}{w'} \equiv \frac{1}{\Delta k_\theta E_2}$. Noting that $k_\theta'^2 - k_\theta^2 = k_\theta''^2 + 2k_\theta k_\theta''$ and making use of Eq.(59),

we have

$$\begin{aligned} & \int_{\text{near } k_\theta^+} \frac{dk_\theta}{|\omega'|} |\phi|^2(k_\theta')(k_\theta'^2 - k_\theta^2) \frac{w'}{x_i'} \frac{2w'}{\Delta'} E_2[(\frac{\omega'' x_i'}{\omega' w'})^2] \\ &= \frac{1}{|\omega|} \frac{w}{x_i} \frac{2w}{\Delta} \int_{-\infty}^{\infty} dk_\theta'' (k_\theta''^2 + 2k_\theta k_\theta'') [|\phi|^2(k_\theta) + \frac{\partial}{\partial k_\theta} |\phi|^2(k_\theta) k_\theta'' + \dots] E_2(\alpha^{+2} k_\theta''^2) \\ &\approx \frac{\sqrt{\pi}}{5} \frac{1}{|\omega|} \frac{w}{x_i} \frac{2w}{\Delta} \frac{1}{\alpha^{+3}} \{|\phi|^2(k_\theta) + 2k_\theta \frac{\partial}{\partial k_\theta} |\phi|^2\} \end{aligned} \quad (60)$$

In the above calculation, $\int_{-\infty}^{\infty} dk_\theta'' k_\theta''^2 E_2(\alpha^{+2} k_\theta''^2) = \frac{\sqrt{\pi}}{5} \frac{1}{\alpha^{+3}}$ has been used, and higher order terms in $\frac{\Delta k_\theta E_2}{\Delta k_\theta}$ have been neglected.

Next, we calculate the nonlocal interaction contribution to γ_i^{nl} . We define $k_\theta'' = k_\theta' - k_\theta^-$. Near k_θ^- , we have $(\frac{\omega'' x_i'}{\omega' w'})^2 \simeq \alpha^{-2} k_\theta''^2$, where $\alpha^- = k_\theta^2 \rho_s^2 |\frac{1-k_\theta^2\rho_s^2}{k_\theta(1+k_\theta^2\rho_s^2)}|\frac{x_i'}{w'}$. Noting that $k_\theta'^2 - k_\theta^2 = (k_\theta^{-2} - k_\theta^2) + 2k_\theta^- k_\theta'' + k_\theta''^2$, and $|\frac{w'}{\omega'} \frac{w'}{x_i'} \frac{w'}{\Delta'}|_{k_\theta^-} = |\frac{w}{\omega} \frac{w}{x_i} \frac{w}{\Delta}|$, we have

$$\begin{aligned} & \int_{\text{near } k_\theta^-} \frac{dk_\theta}{|\omega'|} |\phi|^2(k_\theta')(k_\theta'^2 - k_\theta^2) \frac{w'}{x_i'} \frac{2w'}{\Delta'} E_2[(\frac{\omega'' x_i'}{\omega' w'})^2] \\ &= \frac{1}{|\omega|} \frac{w}{x_i} \frac{2w}{\Delta} \int_{-\infty}^{\infty} dk_\theta'' [(k_\theta^{-2} - k_\theta^2) + 2k_\theta^- k_\theta'' + k_\theta''^2] \\ &\quad \times [|\phi|^2(k_\theta^-) + \frac{\partial}{\partial k_\theta} |\phi|^2(k_\theta^-) k_\theta'' + \dots] E_2(\alpha^{-2} k_\theta''^2) \\ &\approx \frac{1}{|\omega|} \frac{w}{x_i} \frac{2w}{\Delta} (k_\theta^{-2} - k_\theta^2) |\phi|^2(k_\theta^-) \frac{2\sqrt{\pi}}{3} \frac{1}{\alpha^-}, \end{aligned} \quad (61)$$

In the above calculation, $\int_{-\infty}^{\infty} dk_\theta'' E_2(\alpha^{-2} k_\theta''^2) = \frac{2\sqrt{\pi}}{3} \frac{1}{\alpha^-}$ has been used, and high order terms has been neglected as before. Now, combining Eq.(60), and Eq.(61), we obtain the nonlinear transfer rate for ion Compton scattering,

$$\begin{aligned} \frac{\gamma_i^{nl}}{|\omega|} &= \frac{4\pi}{5} \frac{\omega}{\omega_e^*} \frac{T_e}{T_i} (\frac{c}{B})^2 (\frac{k_\theta}{\omega})^2 \frac{r}{q} \frac{w}{x_i} \frac{w}{\Delta} \\ &\quad \times \{ \frac{1}{\alpha^{+3}} \sqrt{k_\theta} \frac{\partial}{\partial k_\theta} [\sqrt{k_\theta} |\phi|^2(k_\theta)] + \frac{5}{3} \frac{1}{\alpha^-} (k_\theta^{-2} - k_\theta^2) |\phi|^2(k_\theta^-) \} \end{aligned} \quad (62)$$

By noting that $\frac{\omega}{\omega_e^*} = \frac{1}{1+k_\theta^2\rho_s^2}$, $k_\theta^{-2} - k_\theta^2 = \frac{1-k_\theta^4\rho_s^4}{k_\theta^2\rho_s^4}$, $(\frac{c}{B})^2 = (\frac{e}{T_e})^2 \rho_s^2 c_s^2$, $\frac{x_i}{\Delta} = \frac{k_\theta \rho_s}{1+k_\theta^2\rho_s^2} \hat{s} \sqrt{\frac{T_e}{T_i}} (\frac{L_s}{L_n})$, the above equation can be rewritten as

$$\frac{\gamma_i^{nl}}{|\omega|} = \frac{4\pi}{5} (\frac{r\hat{s}}{q\rho_s}) (\frac{\Omega_i}{\omega})^2 (\frac{T_e}{T_i})^{\frac{3}{2}} (\frac{L_s}{L_n}) (\frac{w}{x_i})^3 (\frac{e}{T_e})^2$$

$$\times \left\{ \left(\frac{w}{x_i} \right)^2 \frac{(k_\theta \rho_s)^6 (1 + k_\theta^2 \rho_s^2)}{|1 - k_\theta^2 \rho_s^2|^3} \sqrt{k_\theta} \frac{\partial}{\partial k_\theta} [\sqrt{k_\theta} |\phi|^2(k_\theta)] + \frac{5}{3} \text{sign}(1 - k_\theta^2 \rho_s^2) |\phi|^2(k_\theta^-) \right\}. \quad (63)$$

In the above equation, the first term on the right side is the local transfer rate and corresponds to a spectral flow in k_θ space. The second term is the nonlocal transfer rate, which is positive for $k_\theta \rho_s < 1$, and negative for $k_\theta \rho_s > 1$.

b. Nonlinear Transfer Rate Due to Trapped Electron Compton Scattering

In order to evaluate $\gamma_e^{n'}$, let's first calculate the quantity $I_{n'} = |\langle e^{-in'q\theta} \phi_{n'} \rangle_b|^2$. By using Fourier representation in θ for $\phi_{n'}$, i.e. $\phi_{n'} = \sum_{m'} \phi_{n',m'} e^{im'\theta}$, we can write

$$I_{n'} = \sum_{m'} \sum_{p=-\infty}^{\infty} C_{m',m'+p}^{n'} \phi_{n',m'} \phi_{n',m'+p}^*, \quad (64)$$

where the coupling coefficient between different mode rational surface for fixed n' is $C_{m',m'+p}^{n'} = \langle e^{i(m'-n'q)\theta} \rangle_b \langle e^{-i(m'+p-n'q)\theta} \rangle_b$. Since $\langle e^{i(m'-n'q)\theta} \rangle_b$ is localized around a mode rational surface $r_{n',m'}$ with spatial width Δ' , $C_{m',m'+p}^{n'}$ which is centered at $p = 0$ will be a decaying and oscillatory function of p . Therefore, the primary contribution to $I_{n'}$ comes from the $p = 0$ term in Eq.(64). As a matter of fact, it has been shown in Ref.(2) that by keeping all p terms in Eq.(64), $I_{n'}$ is only a factor of $\frac{\pi}{2}$ times that obtained by keeping the $p = 0$ term only. Hence, we may approximate $I_{n'}$ as

$$I_{n'} = \frac{\pi}{2} \sum_{m'} |\phi_{n',m'}|^2 |\langle e^{i(m'-n'q)\theta} \rangle_b|^2 \quad (65)$$

The quantity $\langle e^{i(m'-n'q)\theta} \rangle_b$ can be calculated analytically for $\kappa \ll 1$, since Eq.(52) involves only an integral over $|\langle e^{i(m'-n'q)\theta} \rangle_b|^2$, the answer is not expected to be sensitive to this approximation. Employing $m' - n'q(r) \simeq \frac{x'}{\Delta'}$ yields

$$\langle e^{i(m'-n'q)\theta} \rangle_b \simeq J_0(2\kappa \frac{x'}{\Delta'}) \quad (66)$$

Substituting Eqs.(55), (56), and (66) into Eq.(64), and carrying out the x' integration by noting the relation that $\int_0^{t_0} dt J_0^2(t) \approx \frac{1}{\pi} \ln t_0$ for $t_0 \gg 1$, yields

$$\begin{aligned} I_{n'} &= \frac{\pi}{2} \int_{-w'}^{w'} \frac{dx'}{\Delta'} J_0^2(2\kappa \frac{x'}{\Delta'}) |\phi|^2(k'_\theta) \\ &= \frac{1}{2\kappa} \ln\left(\frac{2\kappa w'}{\Delta'}\right) |\phi|^2(k'_\theta). \end{aligned} \quad (67)$$

Noting that

$$\left| \frac{\partial}{\partial r} \langle e^{-in'q\theta} \phi_{n'} \rangle_b \right|^2 \approx \left(\frac{2\kappa}{\Delta'} \right)^2 |\langle e^{-in'q\theta} \phi_{n'} \rangle_b|^2,$$

and carrying out the κ integration in Eq.(52), we can rewrite the nonlinear transfer rate for trapped electron Compton scattering as:

$$\frac{\gamma_e^{nl}}{|\omega|} \approx \frac{\sqrt{\pi\epsilon} \omega}{|\omega| \omega_e^*} \left(\frac{c}{B} \right)^2 \hat{s}^2 k_\theta^2 \rho_s^2 \frac{\Delta}{x_t} \ln \frac{x_t}{\Delta} \sum_{n'} k_\theta'^2 |\phi|^2(k_\theta') (k_\theta^2 - k_\theta'^2) \delta(\omega - \omega') \ln \frac{w'}{\Delta'}. \quad (68)$$

In arriving at Eq.(68), change of variable $k_\theta' \rightarrow -k_\theta'$ has been made. Now, converting the summation over n' in the above equation into an integral by noting that, $\sum_{n'} = \frac{r}{q} \int dk_\theta'$, and using the relation

$$\delta(\omega_{n'} - \omega_n) = \sum_{j=+,-} \frac{\delta(k_\theta' - k_\theta^j)}{\left| \frac{\partial \omega'}{\partial k_\theta'} \right|} \quad (69)$$

where $k_\theta^+ = k_\theta$ and $k_\theta^- = \frac{1}{k_\theta \rho_s^2}$. we can further simplify the above equation to

$$\begin{aligned} \frac{\gamma_e^{nl}}{|\omega|} &= \sqrt{\pi\epsilon} \frac{\omega}{\omega_e^*} \left(\frac{c}{B} \right)^2 \hat{s}^2 \frac{k_\theta^2 \rho_s^2}{|\omega|} \frac{\Delta}{x_t} \ln \frac{x_t}{\Delta} \\ &\times \frac{r}{q} \int dk_\theta' k_\theta'^2 |\phi|^2(k_\theta') (k_\theta^2 - k_\theta'^2) \ln \frac{w'}{\Delta'} \sum_{j=+,-} \frac{\delta(k_\theta' - k_\theta^j)}{\left| \frac{\partial \omega'}{\partial k_\theta'} \omega(k_\theta^j) \right|} \\ &= \sqrt{\pi\epsilon} \frac{\omega}{\omega_e^*} \left(\frac{c}{B} \right)^2 \hat{s}^2 \frac{k_\theta^2 \rho_s^2}{|\omega|} \frac{\Delta}{x_t} \ln \frac{x_t}{\Delta} \\ &\times \frac{r}{q} k_\theta^{-2} |\phi|^2(k_\theta^-) (k_\theta^2 - k_\theta^{-2}) \ln \frac{w}{\Delta} \frac{1}{\left| \frac{\partial \omega}{\partial k_\theta} \omega(k_\theta^-) \right|} \end{aligned} \quad (70)$$

Replacing k_θ^- with $\frac{1}{k_\theta \rho_s^2}$, and noting that $\left. \frac{\partial \omega}{\partial k_\theta} \right|_{k_\theta^-} = -\frac{c \rho_s}{L_n} \frac{1 - k_\theta^2 \rho_s^2}{1 + k_\theta^2 \rho_s^2}$, after a lengthy but straightforward algebraic manipulation, we obtain the final form for γ_e^{nl} ,

$$\begin{aligned} \frac{\gamma_e^{nl}}{|\omega|} &= -\sqrt{\pi\epsilon} \hat{s}^2 \left(\frac{r \hat{s}}{q \rho_s} \right) \left(\frac{\Omega_i}{\omega} \right)^2 \left(\frac{T_e}{T_i} \right)^{\frac{1}{2}} \left(\frac{L_s}{L_n} \right) \left(\frac{w}{x_i} \right) \\ &\times \left(\frac{\Delta}{x_t} \right) \ln \left(\frac{x_t}{\Delta} \right) \left(\frac{\Delta}{w} \right) \ln \left(\frac{w}{\Delta} \right) \frac{\text{sign}(1 - k_\theta^2 \rho_s^2)}{1 + k_\theta^2 \rho_s^2} \left(\frac{e}{T_e} \right)^2 |\phi|^2(k_\theta^-) \end{aligned} \quad (71)$$

The above equation shows that trapped electron Compton scattering is a nonlocal transfer process. Local interactions ($k_\theta' = k_\theta$) do not contribute because $k_\theta'^2 - k_\theta^2 = 0$.

For Pearlstein-Berk eigenmode structure, we have $w \sim x_i$. Comparing Eqs.(63) and (71), we find that the nonlinear transfer rate due to trapped electron Compton scattering is considerably smaller than that due to ion Compton scattering. This is because: i.) the spectrum of Pearlstein-Berk eigenmode extends to x_i so that ion Compton scattering can take place in a frequency range $\omega + \omega' < k'_{\parallel}(x'_i)v_i \sim \omega'$. However, the trapped electron Compton scattering process is strictly limited by the $\delta(\omega' - \omega)$ function. As a consequence, the local interaction, which is absent in trapped electron Compton scattering process, is very intense in ion Compton scattering. ii.) trapped electron Compton scattering is radially restricted to a very narrow region of width $\Delta \ll x_i$ near mode rational surface while ion Compton scattering extends to x_i . Due to this radial localization effect, the intensity of trapped electron Compton scattering is reduced considerably. This reduction is apparent from Eq.(71), the reduction factor is approximately given by $\frac{\Delta}{x_i} \ln(\frac{x_i}{\Delta}) \frac{\Delta}{x_i} \ln(\frac{x_i}{\Delta}) \sim (\frac{L_n}{L_s})^{\frac{3}{2}} \ll 1$. Therefore, ion Compton scattering, rather than trapped electron Compton scattering is the dominant nonlinear saturation process for the slab-like trapped electron mode.

VII. Saturated Fluctuation Spectrum

In this section, the saturated fluctuation spectrum is calculated. The saturated state is defined by the condition $\frac{\partial}{\partial t} |\phi_n^m|^2 = 0$. From the wave kinetic equation, it implies

$$\gamma_e^l + \gamma^{sd} + \gamma_e^{nl} + \gamma_i^{nl} = 0 \quad (72)$$

namely, the linear growth γ_e^l at each wavenumber k_{θ} is balanced by the combined effect of linear shear damping and the nonlinear transfer due to trapped electron Compton scattering and ion Compton scattering. The trapped electron Compton scattering, which has been shown in last section to be much weaker than the ion Compton scattering, is hereafter neglected. Shear damping can be neglected when we consider the most unstable mode. Consequently, saturation is determined by the balance between the linear growth due to the trapped electron excitation and the nonlinear transfer due to the ion Compton scattering. Shear damping is only important when we consider a linearly marginal stable mode

($\gamma_e^l \leq \gamma^{sd}$), which determines the spectral cutoff. Thus, by neglecting both γ_e^{nl} and γ^{sd} in Eq.(72), the saturation condition can be reduced to,

$$\gamma_i^{nl,c} + \gamma_i^{nl,d} + \gamma_e^l = 0 \quad (73)$$

where $\gamma_i^{nl,c}$ and $\gamma_i^{nl,d}$ are the nonlinear transfer rate due to the local and nonlocal interactions in ion Compton scattering, which corresponds to the first and second term on the right side of Eq.(63), respectively.

Now, let's solve Eq.(73) for fluctuation spectrum at saturation. In the region where $k_\theta \rho_s > 1$, the nonlocal interaction is due to the beating of a high- k_θ and a low- k_θ' fluctuation of similar frequency $\omega \sim \omega'$. The intensity of the interaction is determined by the wave spectrum in region $k_\theta \rho_s < 1$. Due to the nature of the ion Compton scattering process, we can anticipate that for even moderate long wavelength fluctuation levels, the nonlocal interaction is strong and causes a nonlinear transfer rate which exceeds the growth rate due to trapped electron excitation. As a consequence, these high- k_θ modes are only very feebly excited (if at all), and thus do not contribute significantly to either the fluctuation level or the transport. Thus, the spectrum is populated only for $k_\theta \rho_s < 1$.

In region $k_\theta \rho_s < 1$, the nonlocal interaction is negligible. The remainder of Eq.(73) is then a local first order differential equation and can be easily solved. In order to simplify the analysis, we introduce a new variable $\bar{k}_\theta \equiv k_\theta \rho_s$. With \bar{k}_θ , we can rewrite $\gamma_i^{nl,c}$ and γ_e^l as

$$\begin{aligned} \frac{\gamma_i^{nl,c}}{|\omega|} &= \frac{4\pi}{5} \left(\frac{r\hat{s}}{q\rho_s} \right) \left(\frac{L_n}{\rho_s} \right)^2 \left(\frac{T_e}{T_i} \right)^{\frac{3}{2}} \left(\frac{L_s}{L_n} \right) \left(\frac{w}{x_i} \right)^5 \left(\frac{e}{T_e} \right)^2 \bar{k}_\theta^4 \sqrt{\bar{k}_\theta} \frac{\partial}{\partial \bar{k}_\theta} [\sqrt{\bar{k}_\theta} |\phi|^2(\bar{k}_\theta)] \\ &\equiv A_i^{nl} \bar{k}_\theta^4 \sqrt{\bar{k}_\theta} \frac{\partial}{\partial \bar{k}_\theta} [\sqrt{\bar{k}_\theta} |\phi|^2(\bar{k}_\theta)] \end{aligned} \quad (74)$$

where A_i^{nl} , which measures the intensity of ion Compton scattering, is given by

$$A_i^{nl} = \frac{4\pi}{5} \left(\frac{r\hat{s}}{q\rho_s} \right) \left(\frac{L_n}{\rho_s} \right)^2 \left(\frac{T_e}{T_i} \right)^{\frac{3}{2}} \left(\frac{L_s}{L_n} \right) \left(\frac{w}{x_i} \right)^5 \left(\frac{e}{T_e} \right)^2 \quad (75)$$

also

$$\begin{aligned}\frac{\gamma_e^l}{|\omega|} &= \sqrt{\epsilon} \left(\frac{L_n}{L_s}\right)^{\frac{1}{2}} \ln\left(\frac{x_t}{\Delta}\right) \bar{k}_\theta \frac{\bar{\gamma}(\bar{k}_\theta)}{\hat{s}} \\ &\equiv A_e^l \bar{k}_\theta \frac{\bar{\gamma}(\bar{k}_\theta)}{\hat{s}}\end{aligned}\quad (76)$$

where A_e^l and $\bar{\gamma}(\bar{k}_\theta)$ are defined by

$$A_e^l = \sqrt{\epsilon} \left(\frac{L_n}{L_s}\right)^{\frac{1}{2}} \ln\left(\frac{x_t}{\Delta}\right) \quad (77)$$

$$\bar{\gamma}(\bar{k}_\theta) = \frac{1}{2\sqrt{\pi}} \text{Im} g_n, \quad (78)$$

Thus, the saturation condition is given by the following equation,

$$A_i^{nl} \bar{k}_\theta^4 \sqrt{\bar{k}_\theta} \frac{\partial}{\partial \bar{k}_\theta} [\sqrt{\bar{k}_\theta} |\phi|^2(\bar{k}_\theta)] + A_e^l \bar{k}_\theta \frac{\bar{\gamma}(\bar{k}_\theta)}{\hat{s}} = 0. \quad (79)$$

The solution of the above equation is

$$|\phi|^2(\bar{k}_\theta) = \frac{1}{\sqrt{\bar{k}_\theta}} |\phi|^2(1) - \frac{1}{\sqrt{\bar{k}_\theta}} \frac{A_e^l}{A_i^{nl}} \int_1^{\bar{k}_\theta} \bar{k}'_\theta^{-\frac{7}{2}} \frac{\bar{\gamma}(\bar{k}'_\theta)}{\hat{s}} d\bar{k}'_\theta \quad (80)$$

In order to evaluate the integral in the above equation, a specific instability drive $\bar{\gamma}(\bar{k}_\theta)$ must be utilized. For simplicity, $|\phi|^2(1)$ is neglected by setting $\bar{k}_\theta = 1$ to be the upper wavenumber cutoff of the spectrum, because $|\phi|^2(\bar{k}_\theta)$ falls off rapidly for $\bar{k}_\theta > 1$. As the calculations are straightforward, we just present the results (for $\bar{k}_\theta < 1$) for different collisionality regimes.

1. Collisionless Regime

$$\bar{\gamma}(\bar{k}_\theta) \simeq \bar{\gamma}^c$$

$$\bar{\gamma}^c = \epsilon_n^{-\frac{3}{2}} e^{-\frac{1}{\epsilon_n}}$$

$$|\phi|^2(\bar{k}_\theta) \simeq \frac{2}{5} \frac{A_e^l}{A_i^{nl}} \frac{\bar{\gamma}^c}{\hat{s}} \bar{k}_\theta^{-3} I^c(\bar{k}_\theta) \quad (81)$$

with $\epsilon_n = \frac{L_n}{R}$, and $I^c(\bar{k}_\theta) = 1 - \bar{k}_\theta^{\frac{5}{2}}$.

2. Dissipative Regime

$$\begin{aligned}
 \bar{\gamma}(\bar{k}_\theta) &\simeq \bar{\gamma}^d \bar{k}_\theta \\
 \bar{\gamma}^d &= \frac{c_s}{\nu_{eff} L_n} \\
 |\phi|^2(\bar{k}_\theta) &\simeq \frac{2}{5} \frac{A_e^l}{A_i^l} \frac{\bar{\gamma}^d}{\hat{s}} \bar{k}_\theta^{-2} I^d(\bar{k}_\theta)
 \end{aligned} \tag{82}$$

where $I^d(\bar{k}_\theta) = 1 - \bar{k}_\theta^{\frac{3}{2}}$.

Eqs.(81), (82) predict a power law spectrum, $|\phi|^2(k_\theta) \sim k_\theta^{-\alpha}$, where $\alpha=2$ and 3 for dissipative and collisionless trapped electron modes, respectively. This spectrum is drawn schematically in Fig.3 which shows the lower cutoff \bar{k}_θ^c and upper cutoff 1. On the same picture, we also show the schematic of the linear growth rate so that one can see that the saturated spectrum is down-shifted towards the lower k_θ region as a consequence of ion Compton scattering. With the spectrum intensity we obtained above, we can calculate the fluctuation level and steady state transport coefficients. Here, the fluctuation level will be calculated, while the calculation of the transport coefficients is left for next section.

The fluctuation level is defined as

$$\begin{aligned}
 \langle \left(\frac{\tilde{n}}{n_0} \right)^2 \rangle &\simeq \langle \left(\frac{e\phi}{T_e} \right)^2 \rangle \\
 &= \sum_n \left| \frac{e}{T_e} \phi_n^m \right|^2 \equiv \left(\frac{e}{T_e} \right)^2 \frac{r}{q} \int \frac{dk_\theta}{\Delta} \int_{r-x_i}^{r+x_i} dr_n |\phi_n^m|^2
 \end{aligned} \tag{83}$$

where the bracket means an average over θ and ξ . By carrying out the r_n integration, and noting that $\frac{x_i}{\Delta} = \hat{s}(k_\theta \rho_s) \frac{L_s}{L_n} \sqrt{\frac{T_e}{T_i}}$, we have

$$\langle \left(\frac{e\phi}{T_e} \right)^2 \rangle = 4 \left(\frac{T_e}{T_i} \right)^{\frac{1}{2}} \frac{L_s}{L_n} \left(\frac{e}{T_e} \right)^2 \frac{r \hat{s}}{q \rho_s} \int_{\bar{k}_\theta^c}^1 \bar{k}_\theta |\phi|^2(\bar{k}_\theta) d\bar{k}_\theta \tag{84}$$

In the above equation, the upper cutoff of the spectrum has been set to be 1, and the lower cutoff \bar{k}_θ^c is determined by the balance between the linear growth rate due to trapped electron excitation and the shear damping rate, i.e.

$$A_e^l \bar{k}_\theta^c \frac{\bar{\gamma}(\bar{k}_\theta^c)}{\hat{s}} = \frac{L_n}{L_s} \tag{85}$$

A more accurate determination of \bar{k}_θ^c should include the nonlinear transfer rate in the balance equation above which could result in a cutoff smaller than that determined from Eq.(85), i.e. some linearly stable modes will be nonlinearly excited. However, this excitation is very weak, since for small \bar{k}_θ the nonlinear transfer rate is very small. Therefore the difference between the rigorous lower cutoff and \bar{k}_θ^c determined from Eq.(85) can be ignored. Now, substituting the steady state spectrum in Eqs.(81),(82) and noting Eqs.(75) and (77), the fluctuation level in various collisionality regimes can be readily calculated. The results are

$$\langle (\frac{e\phi}{T_e})^2 \rangle \simeq 0.6 \frac{T_i}{T_e} (A_e^l \frac{\bar{\gamma}}{s}) G(\bar{k}_\theta^c) (\frac{\rho_s}{L_n})^2 \quad (86)$$

In obtaining the above result, the spatial width of the spectrum w has been set equal to x_i . In the above equation, $\bar{\gamma}$ accounts for the linear growth rate in different collisionality regime and is given by

$$\bar{\gamma} = \begin{cases} \epsilon_n^{-\frac{3}{2}} e^{-\frac{1}{\epsilon_n}}, & \text{collisionless regime;} \\ \frac{c_s}{\nu_{eff} L_n}, & \text{dissipative regime;} \end{cases} \quad (87)$$

and $G(\bar{k}_\theta^c)$ is the function that represents the effects of the spectrum shape and cutoff,

$$G(\bar{k}_\theta^c) = \begin{cases} \frac{1}{\bar{k}_\theta^c} - \frac{5}{3} + \frac{2}{3} \bar{k}_\theta^c \frac{3}{2}, & \text{collisionless regime;} \\ \ln \frac{1}{\bar{k}_\theta^c} - \frac{2}{3} + \frac{2}{3} \bar{k}_\theta^c \frac{3}{2}, & \text{dissipative regime.} \end{cases} \quad (88)$$

Since $A_e^l \propto \sqrt{\frac{L_n}{L_s}}$, Eq.(86) shows that the fluctuation level predicted is well below the mixing length type estimate of $\frac{e\phi}{T_e} \sim \frac{x_i}{L_n} \sim \sqrt{\frac{L_s}{L_n}} \frac{\rho_s}{L_n}$. This is due to the contribution of the radial wavenumbers $k_r^l \sim \mu' x_i \sim \sqrt{\frac{L_s}{L_n}} x_i^{-1} > x_i^{-1}$ to the nonlinear coupling coefficient $\vec{k} \cdot \vec{k}' \times \vec{z}$ (since the slab-like eigenmode spectrum extends to x_i), and the weak turbulence reduction factor $\langle \frac{\gamma_e^l}{\omega_k} \rangle_{\vec{k}} \sim A_e^l \frac{\bar{\gamma}}{s} \ll 1$. Here, $\langle \dots \rangle_{\vec{k}}$ represents spectrum average.

VIII. Turbulent Transport

Having obtained the wave number spectrum and the fluctuation level, we now consider the effect of trapped electron mode driven turbulence on particle and heat transport.

The turbulent particle and heat flux are determined by the correlation of the fluctuating radial velocity with the density and pressure fluctuation respectively, i.e.

$$\Gamma_j = \langle \tilde{V}_r \tilde{n}_j \rangle, \quad (89)$$

$$Q_j = \langle \tilde{V}_r \tilde{p}_j \rangle. \quad (90)$$

The bracket represents an ensemble average which in practice can be replaced by an average over the fast variation variables θ and ξ .

For the particle flux, the quasineutrality condition also implies that the particle transport is ambipolar, i.e. the spatial width averaged electron flux should be equal to the ion flux, $\Gamma_e = \Gamma_i$. In the following, we calculate the electron particle flux directly using the quasi-linear approximation. This is valid because the trapped electron nonlinear wave-particle interaction is very weak and does not contribute to the saturation criterion. From Eq. (89), the electron particle flux can be rewritten as

$$\begin{aligned} \Gamma_e &= -\frac{c}{B} \sum_n k_\theta \text{Im}(\tilde{n}_n^{e(1)} \tilde{\phi}_{-n}^-) \\ &\equiv -\frac{c}{B} \frac{r}{q} \int \frac{dk_\theta}{\Delta} \int_{r-x_t}^{r+x_t} dr_n k_\theta \text{Im}(\tilde{n}_n^{e(1)} \tilde{\phi}_{-n}^-) \end{aligned} \quad (91)$$

Note in the above equation, the limits for the r_n integral have been set to be $r \pm x_t$ in order to ensure satisfaction of the well-known relationship between the quasilinear equation and $\text{Im}\epsilon$, and preservation of spectrum width averaged ambipolarity. The particle diffusion coefficient is defined as

$$D = -\frac{\Gamma}{\frac{dN}{dr}} \quad (92)$$

Substituting Eqs.(10a) and (10b) for $\tilde{n}_n^{e(1)}$ in Eq.(91), and making use of the spectrum function $|\phi|^2(k_\theta)$ at steady state, we can obtain the particle diffusion coefficient D . The result is

$$D = 0.4 \left(\frac{T_i}{T_e}\right)^{\frac{3}{2}} \left(\frac{L_n}{L_s}\right)^{\frac{1}{2}} (A_e^l \frac{\bar{\gamma}}{s})^2 F(\bar{k}_\theta) \frac{c_s \rho_s^2}{L_n} \quad (93)$$

where the function $F(\bar{k}_\theta^c)$ is given by

$$F(\bar{k}_\theta^c) = \begin{cases} \frac{5}{7} - \bar{k}_\theta^c + \frac{2}{7} \bar{k}_\theta^{c\frac{7}{2}}, & \text{collisionless regime,} \\ \frac{1}{15} - \frac{1}{5} \bar{k}_\theta^{c3} + \frac{2}{15} \bar{k}_\theta^{c\frac{9}{2}}, & \text{dissipative regime.} \end{cases}$$

and the instability source term $\bar{\gamma}$ is given by Eq. (87).

Now let's turn to the discussion of the heat transport. From Eq.(90), the heat flux can be rewritten as,

$$Q^j = -\frac{c}{B} \sum_n k_\theta \text{Im}[(\tilde{p}_n^{j(1)} + \tilde{p}_n^{j(3)} + \dots) \tilde{\phi}_{-n}^j] \quad (94)$$

where $\tilde{p}_n^{j(l)}$ is the l th order pressure response in the weak turbulence expansion. The first term in the above equation corresponds to the quasilinear heat flux. The second term corresponds to the heat flux caused by nonlinear wave-particle interaction. For electrons, the quasilinear flux is dominant, since nonlinear trapped electron-wave interaction is weak. For ions, the ion Compton scattering induced heat flux is dominant, since the quasilinear flux caused by the shear damping is negligible. As a consequence, we can write the thermal flux for ions and electrons as:

$$Q^i = -\frac{c}{B} \sum_n k_\theta \text{Im}(\tilde{p}_n^{i(3)} \tilde{\phi}_{-n}^i) \quad (95a)$$

$$Q^e = -\frac{c}{B} \sum_n k_\theta \text{Im}(\tilde{p}_n^{e(1)} \tilde{\phi}_{-n}^e) \quad (95b)$$

where $\tilde{p}_n^{i(3)}$ and $\tilde{p}_n^{e(1)}$ are given by

$$\tilde{p}_n^{i(3)} = \int d^3 \vec{v} J_0 \left(\frac{k_\perp v_\perp}{\Omega_i} \right) \frac{1}{2} m_i v^2 \hat{h}_n^{i(3)} \quad (96a)$$

$$\tilde{p}_n^{e(1)} = \int_{-\pi}^{\pi} \frac{d\theta}{2\pi} e^{i(nq-m)\theta} \int_t d^3 \vec{v} \frac{1}{2} m_e v^2 \hat{h}_n^{e(1)} \quad (96b)$$

The thermal flux defined as above can be divided into two terms,

$$Q^j = Q_{cv}^j + Q_{cd}^j$$

On the right side of the above equation, the first term Q_{cv}^j is called convected thermal flux, and is driven by the density gradient. Since this term results from the transport of heat by particle diffusion, we may write this term as $Q_{cv}^j = T_j \Gamma$. The second term Q_{cd}^j is called the conducted thermal flux. It is driven by the temperature gradient. We define the heat transport coefficient χ_j by

$$\chi_j = -\frac{Q_{cd}^j}{N \frac{dT_j}{dr}} \quad (97)$$

Note that in order to calculate the thermal transport coefficients, finite temperature gradients are required. The transport coefficients determined in this way usually are nonlinear functions of the temperature gradient since the linear growth rate γ_e^l also depends on the ∇T_e . For self-consistency, strictly speaking, we must require that the temperature gradients we introduce to calculate the thermal transport coefficients be relatively weak so that our previous assumptions are not violated. In such cases, the transport coefficients do not depend strongly on the temperature gradient. Now substituting $h_m^{i(3)}$ from Eq.(34a) and $\hat{h}_n^{e(1)}$ from Eq.(8b) into the Eqs.(95b) and (96b) and carrying out the velocity integrals, we can obtain the third order ion pressure response and the first order electron pressure response. Substituting these responses into Eqs.(95a) and (95b), and noting the definition for χ_j in Eq.(97), we obtain

$$\chi^i = 0.8 \left(\frac{T_i}{T_e}\right)^{\frac{3}{2}} \left(\frac{L_n}{L_s}\right)^{\frac{1}{2}} (A_e^l \bar{\gamma})^2 F(\bar{k}_\theta^c) \frac{\rho_s^2 c_s}{L_n} \quad (98)$$

$$\chi^e = 0.8 \left(\frac{T_i}{T_e}\right)^{\frac{3}{2}} \left(\frac{L_n}{L_s}\right)^{\frac{1}{2}} (A_e^l \bar{\gamma})^2 H(\bar{k}_\theta^c) \frac{c_s \rho_s^2}{L_n} \quad (99)$$

where $H(\bar{k}_\theta^c)$ is given by

$$H(\bar{k}_\theta^c) = \begin{cases} \frac{1}{\epsilon_n} \left[\left(\frac{1}{\epsilon} - \frac{3}{2} \right) G(\bar{k}_\theta^c) - \frac{3}{2} F(\bar{k}_\theta^c) \right], & \text{for collisionless mode} \\ \frac{1}{\pi} [25F(\bar{k}_\theta^c) + 9\bar{k}_\theta^c G(\bar{k}_\theta^c)], & \text{for dissipative mode.} \end{cases}$$

For trapped electron driven drift wave turbulence, the momentum diffusivity $\chi_\phi \simeq \chi_i$. The particle transport coefficient, the heat transport coefficients shown in Eqs.(93), (98), (99) are substantially smaller than the mixing length type estimate. This is due to the effect

that trapped electron response is radially localized to $x \leq \Delta < x_t$, the weak turbulence reduction factor $\langle \frac{\gamma_e^i}{\omega_k} \rangle_k^2$, and the reduction in the fluctuation level which results from the enhanced ion Compton scattering.

Now, let's discuss the practical implications of Eq.(93), (98) and (99) for tokamak transport. First, we notice that $L_s = \hat{s}^{-1}qR$ and $A_e^i \propto (\frac{L_n}{L_s})^{\frac{1}{2}}$. Hence,

$$D, \chi_e, \chi_i \propto \left(\frac{\hat{s} L_n}{q R} \right)^{\frac{3}{2}}$$

i.e. all the transport coefficients have favorable major radius dependence. This favorable major radius dependence results from the radial localization of trapped electron response, and therefore will occur in all collisionality regimes. Second, in the dissipative regime, $\bar{\gamma} = \frac{c_s}{L_n \nu_{eff}} \propto T_e^2 m_i^{-\frac{1}{2}} n^{-1}$, $c_s \rho_s \propto m_i^{\frac{1}{2}} T_e^{\frac{3}{2}}$, we have,

$$D \sim \chi_e \sim \chi_i \propto T_e^{\frac{11}{2}} n^{-2} m_i^{-\frac{1}{2}}$$

i.e. all the transport coefficients in the dissipative regime have a favorable dependence on both the density and the ion mass. These favorable dependences do not occur in the collisionless regime. Third, we observe the manifestation of confinement improvement in peaked profile, collisionless regimes. This is apparent from the dependence of the transport coefficients on $\exp(-\frac{R}{L_n})$, which is fundamental to the collisionless trapped electron growth rate.

IX. Discussion and Conclusion

In this paper, a kinetic theory of trapped electron driven drift wave turbulence which treats electron and ion nonlinearity on an equal footing is presented. The principal results of this investigation are summarized in Table I. In particular, we find:

- i.) the disparity between the basic scales $\Delta < x_t < x_i$ indicates that ion Compton scattering is the dominant nonlinear process for slab-like trapped electron driven drift wave turbulence.

-
- ii.) ion Compton scattering induces spectral transfer to long wavelengths. The resulting spectrum $|\phi|^2(k_\theta) \sim k_\theta^{-\alpha}$ ($\alpha=2$ and 3 for dissipative and collisionless regimes, respectively) is heavily damped for $k_\theta \rho_s > 1$ and cutoff by shear damping at \bar{k}_θ^c .
 - iii.) saturated fluctuation levels are smaller than those predicted by naive mixing length theory $\frac{e\phi}{T_e} \sim \frac{x_t}{L_n} \sim \sqrt{\frac{L_e}{L_n} \frac{\rho_s}{L_n}}$. This disparity is due to the appearance of $k_r' \rho_i \sim 1$ contributions to the coupling coefficient $\vec{k} \cdot \vec{k}' \times \vec{e}_\parallel$ and to the effects of "weak turbulence" factors $\langle \frac{\gamma_e'}{\omega_k} \rangle_{\vec{k}} \sim A_e^I \frac{\bar{\gamma}}{\bar{\omega}} \ll 1$.
 - iv.) the transport coefficients χ_e , χ_i , and D have been determined using the calculated fluctuation spectrum. The results manifest explicit dependence on the spectral shape and cutoffs, and are smaller than the mixing length estimate predictions due to effects of localization of the trapped electron response to $\Delta(< x_t < x_i)$, the "weak turbulence" factor $(A_e^I \frac{\bar{\gamma}}{\bar{\omega}})^2$ and the reduction in fluctuation levels discussed above.

These results have a number of interesting implications for tokamak confinement theory, which include:

- i.) the appearance of the robust favorable major radius scaling, due to the trapped electron layer localization effect.
- ii.) the manifestation of favorable isotope scaling in the dissipative trapped electron regime. This favorable isotope scaling is accompanied by a transition from $\chi \sim 1/n$ to $\chi \sim 1/n^2$ scaling.
- iii.) the manifestation of confinement improvement in the peaked profile, collisionless trapped electron regime. This trend is a direct consequence of the $\exp(-\frac{R}{L_n})$ dependence of the collisionless trapped electron mode growth rate.
- iv.) finally (and most important!), we observed that short wavelength drift wave turbulence levels and transport coefficients are considerably smaller than predictions derived from naive mixing length estimates. This result suggests that longer wavelength toroidal drift waves and trapped ion modes are probably the dominant agents for electron driven core transport in tokamaks.

At this point, it is appropriate to briefly comment on the implications of this work for longer wavelength, toroidicity-induced trapped electron mode turbulence. In contrast to the slab-like branch, toroidal modes are standing waves, with coupled poloidal sub-harmonics of width $\Delta x \leq \frac{1}{k_\theta s}$ and $k_\parallel v_i \ll \omega$. It is apparent from the analysis presented in this paper that: (a) ion Compton scattering is ineffectual for toroidal modes, since $\Delta(k_\parallel v_i) \ll \omega$. (b) the role of electron-mediated and ion-mediated nonlinearity are comparable, since $\Delta x \sim \Delta$. (c) it is likely that $\vec{E} \times \vec{B}$ mode coupling is the dominant ion-mediated nonlinear process, since $k_\perp^2 \rho_s^2 \ll 1$ for toroidal drift wave¹². In contrast to the “conventional wisdom”, it is easily seen that such $\vec{E} \times \vec{B}$ mode coupling transfers energy to small scales, even in quasi-two dimensional systems.¹⁶ In combination with the trapped electron mediated transfer to large k_θ discussed in this paper, such ion mode coupling suggests the energy flow in long wavelength drift wave turbulence is toward *small* scales. A detailed theoretical analysis of toroidicity induced drift wave turbulence is underway and will be reported in a future publication.

We want to remark that in our calculation the electron temperature gradient effect has been neglected. Finite electron temperature gradient can enhance the linear growth rate¹, but will not change the trapped electron dynamics. Since the linear theory will change when finite η_e is included, the steady state spectra can be expected to change, as well. However, our results obtained in this paper can be easily modified to include this change.

Finally, the results presented here further underscore the need for gyrokinetic¹⁷ and bounce-kinetic¹⁵ simulations of trapped electron mode turbulence. Similarly, coupled fluctuation and transport studies of low frequency turbulence, particularly in flexible magnetic configurations such as stellarators,¹⁸ should be vigorously pursued.

Acknowledgments

This work was supported by the U. S. Department of Energy under Grant No. DE-FG05-50388 with the University of Texas at Austin and Grant No. DE-FG03-50388-53275

with the University of California, San Diego. P. H. Diamond would like to acknowledge support from an Alfred P. Sloan Research Fellowship and a National Science Foundation Presidential Young Investigator Award.

References

1. W. M. Tang, *Nuclear Fusion* **18**, 1089 (1978).
2. P. J. Catto, and K. T. Tsang, *Phys. Fluids* **21**, 1381 (1978).
3. W. M. Manheimer, K. R. Chu, E. Ott, and J. P. Boris, *Phys. Rev. Lett.* **37**, 286 (1976).
4. A. Rogister, and G. Hasselberg, *Phys. Fluids* **26**, 1467 (1983).
5. P. L. Similon, and P. H. Diamond, *Phys. Fluids* **27**, 916 (1984).
6. L. Chen, R. L. Berger, J. G. Lominadze, M. N. Rosenbluth, and P. H. Rutherford, *Phys. Rev. Lett.* **39**, 754 (1977).
7. P. H. Diamond, P. L. Similon, P. W. Terry, C. W. Horton, S. M. Mahajan, J. D. Meiss, M. N. Rosenbluth, K. Swartz, T. Tajima, R. D. Hazeltine, D. W. Ross, in *Plasma Physics and Controlled Nuclear Fusion Research* (IAEA, Vienna, 1982), Vol.I, p.259.
8. R. Waltz, *Phys. Fluids* **28**, 577 (1985).
9. A. Hasegawa, and K. Mima, *Phys. Fluids* **21**, 87 (1978).
10. T. Tange, K. Nishikawa, and A. K. Sen, *Phys. Fluids* **25**, 1592 (1982).
11. L. D. Pearlstein, and H. L. Berk, *Phys. Rev. Lett.* **23**, 220 (1969).
12. L. Chen, and C. Z. Cheng, *Phys. Fluids* **23**, 2242 (1980).
13. R. Z. Sagdeev and A. A. Galeev, in *Nonlinear Plasma Theory*, edited by T. M. O'Neil and D. L. Book (Benjamin, New York, 1969), p.89.
14. E. A. Frieman, and L. Chen, *Phys. Fluids* **25**, 502 (1982).
15. F. Y. Gang, and P. H. Diamond, submitted to *Phys. Fluids B* May, 1990.
16. P. H. Diamond, and H. Biglari, submitted to *Phys. Rev. Lett.* June, 1990.
17. W. W. Lee, *Phys. Fluids* **26**, 556 (1983).
18. B. A. Carreras, N. N. Dominguez, P. H. Diamond, and L. Garcia, *Bull. Am. Phys. Soc.* **34**. 2046 (1989).

Table I. Summary of Principal Results

Quantities	Collisionless Regime ($\omega > \omega_{de} > \nu_{eff}$)	Dissipative Regime ($\nu_{eff} > \omega > \omega_{de}$)
$\bar{\gamma}$	$\epsilon_n^{-\frac{3}{2}} e^{-\frac{1}{\epsilon_n}}$	$\frac{c_s}{\nu_{eff} L_n}$
$ \phi ^2(\bar{k}_\theta)$	$0.4 \frac{A_e^1}{A_e^1} \frac{\bar{\gamma}}{s} \bar{k}_\theta^{-3} I(\bar{k}_\theta)$	$0.4 \frac{A_e^1}{A_e^1} \frac{\bar{\gamma}}{s} \bar{k}_\theta^{-4} I(\bar{k}_\theta)$
$(\frac{\bar{n}}{n_0})^2$	$0.6 \frac{T_i}{T_e} (A_e^1 \frac{\bar{\gamma}}{s}) G(\bar{k}_\theta^c) (\frac{\rho_s}{L_n})^2$	same
D	$0.4 (\frac{T_i}{T_e})^{\frac{3}{2}} (\frac{L_n}{L_s})^{\frac{1}{2}} (A_e^1 \frac{\bar{\gamma}}{s})^2 F(\bar{k}_\theta^c) \frac{c_s \rho_s^2}{L_n}$	same
χ_i	$0.8 (\frac{T_i}{T_e})^{\frac{3}{2}} (\frac{L_n}{L_s})^{\frac{1}{2}} (A_e^1 \frac{\bar{\gamma}}{s})^2 F(\bar{k}_\theta^c) \frac{c_s \rho_s^2}{L_n}$	same
χ_e	$0.8 (\frac{T_i}{T_e})^{\frac{3}{2}} (\frac{L_n}{L_s})^{\frac{1}{2}} (A_e^1 \frac{\bar{\gamma}}{s})^2 H(\bar{k}_\theta^c) \frac{c_s \rho_s^2}{L_n}$	same
$I(\bar{k}_\theta)$	$1 - \bar{k}_\theta^{\frac{5}{2}}$	$1 - \bar{k}_\theta^{\frac{3}{2}}$
$G(\bar{k}_\theta^c)$	$\frac{1}{\bar{k}_\theta^c} - \frac{5}{3} + \frac{2}{3} \bar{k}_\theta^{\frac{3}{2}}$	$\ln \frac{1}{\bar{k}_\theta^c} - \frac{2}{3} + \frac{2}{3} \bar{k}_\theta^{\frac{3}{2}}$
$F(\bar{k}_\theta^c)$	$\frac{5}{7} - \bar{k}_\theta^c + \frac{2}{7} \bar{k}_\theta^{\frac{7}{2}}$	$\frac{1}{15} - \frac{1}{5} \bar{k}_\theta^c + \frac{2}{15} \bar{k}_\theta^{\frac{3}{2}}$
$H(\bar{k}_\theta^c)$	$\frac{1}{\epsilon_n} [(\frac{1}{\epsilon_n} - \frac{3}{2}) G(\bar{k}_\theta^c) - \frac{3}{2} F(\bar{k}_\theta^c)]$	$\frac{1}{\pi} [25 F(\bar{k}_\theta^c) + 9 \bar{k}_\theta^c G(\bar{k}_\theta^c)]$
\bar{k}_θ^c	$\frac{L_n}{L_s} \frac{s}{A_e^1 \bar{\gamma}} \propto (\frac{L_n}{L_s})^{\frac{1}{2}}$	$(\frac{L_n}{L_s} \frac{s}{A_e^1 \bar{\gamma}})^{\frac{1}{2}} \propto (\frac{L_n}{L_s})^{\frac{1}{4}}$

Figure Captions

Figure 1: This figure depicts the linear eigenmode structure of a slab-like drift wave (Pearlstein-Berk outgoing wave) with three different spatial scale lengths Δ , x_t , and x_i . Two neighbouring mode rational surface of $(\frac{m}{n})$ and $(\frac{m+1}{n})$ are also shown on the diagram.

Figure 2: This figure depicts the linear dispersion relation for slab-like drift mode. On the diagram, two distant wavenumbers k_θ and $1/k_\theta \rho_s^2$, which correspond to the same frequency $\omega(k_\theta)$, are shown.

Figure 3: This figure depicts the shape and cutoffs of the saturated spectrum $|\phi|^2(k_\theta)$. \bar{k}_θ^c is the lower cutoff determined by the balance between the linear growth rate and the shear damping rate. On the same diagram, the schematic curve of the linear growth rate is also shown.